Annu. Rev. Nucl. Particle Science 2007 57

What Do Electromagnetic Plasmas Tell Us about Quark-Gluon Plasma?

Stanisław Mrówczyński
Institute of Physics, Świętokrzyska Academy,
ul. Świętokrzyska 15, PL - 25-406 Kielce, Poland
and Sołtan Institute for Nuclear Studies,
ul. Hoża 69, PL - 00-681 Warsaw, Poland
e-mail: mrow@fuw.edu.pl

Markus H. Thoma
Max-Planck-Institute for Extraterrestrial Physics,
P.O. Box 1312, D - 85741 Garching, Germany
e-mail: mthoma@mpe.mpg.de

arXiv:nucl-th/0701002v1 31 Dec 2006

Key Words Quark-Gluon Plasma, Relativistic Heavy-Ion Collisions

Abstract
Since the quark-gluon plasma (QGP) reveals some obvious similarities to the well-known electromagnetic plasma (EMP), an accumulated knowledge on EMP can be used in the QGP studies. After discussing similarities and differences of the two systems, we present theoretical tools which are used to describe the plasmas. The tools include: kinetic theory, hydrodynamic approach and diagrammatic perturbative methods. We consider collective phenomena in the plasma with a particular emphasis on instabilities which crucially influence temporal evolution of the system. Finally, properties of strongly coupled plasma are discussed.

CONTENTS

INTRODUCTION 2

THEORETICAL TOOLS 4
Transport theory 4
Hydrodynamic approach 7
Diagrammatic methods 12

COLLECTIVE PHENOMENA 14
Screening 14
Collective modes 15
Instabilities 18
Energy loss 23

STRONGLY COUPLED PLASMAS 25

1 INTRODUCTION

The plasma - the ionized gas of electrons and ions - has been actively studied since its discovery in a discharge tube at the end of 19-th century. The term *plasma* was introduced by Irving Langmuir in 1929. Prospects to get a practically unlimited source of energy due to nuclear fusion reactions in a hot ionized gas of hydrogen isotopes, have stimulated a large scale program to study plasmas in terrestrial experiments for over half a century. Plasmas are also actively studied by astrophysicists as it appears the most common phase of matter. About 99% of the entire visible Universe is in the plasma phase, not only stars are formed of ionized gas but the interstellar and intergalactic medium is also a plasma, although a very sparse one. Principles of the plasma physics can be found in e.g. the well-known textbooks (1, 2).

The quark-gluon plasma (QGP) is the system of quarks and gluons which are not confined in hadron's interiors but can freely move in a whole volume occupied by the system. A broad presentation of the whole field of QGP physics is contained in three volumes of review articles (3, 4, 5); the lectures (6) can serve as an elementary introduction. Active studies of QGP started in the mid 1980s when relativistic heavy-ion collisions offered an opportunity to create a drop of QGP in a laboratory. The experimental programs at CERN and BNL provided an evidence of the QGP production at the early stage of nucleus-nucleus collisions, when the system is extremely hot and dense, but properties of QGP remain enigmatic. So, one can ask: what do electromagnetic plasmas (EMP) tells us about QGP?

The QGP reveals some obvious similarities to the well-known electromagnetic plasma, as Quantum Chromodynamics (QCD) describing the interactions of the quarks and gluons resembles Quantum Electrodynamics (QED) which governs interactions of charged objects. Thus, some lessons from EMP should be useful in the exploration of QGP. The aim of this article is to discuss what QGP physicists can actually learn from their EMP colleagues and how the huge accumulated knowledge on EMP can be used in the QGP studies. However, we have to be aware not only of similarities but of important differences between EMP and QGP. Some differences are of rather trivial origin but some are deeply rooted in dynamical foundations of the two systems.

Let us enumerate these 'trivial' dissimilarities. QGP is usually relativistic or even ultrarelativistic while EMP is mostly nonrelativistic in laboratory experiments. The differences between the non-relativistic and relativistic plasmas go far beyond the kinematics of motion of plasma particles. For example, let us consider the plasma's composition. In the non-relativistic system, there are particles but no antiparticles and the particle's number is conserved. In the relativistic system we have both particles andantiparticles, as electrons and positrons in EMP, and the lepton number - not the particle's number - is conserved. Particle number density is not a right quantity to characterize the system. For this reason, the

QGP physicists use the baryon and strangeness densities.

Another 'trivial' but very important distinctive feature of EMP is the huge mass difference between electrons and ions which is responsible for a specific dynamic role of heavy ions. The ions are usually treated as a passive background, which merely compensates the charge of electrons, but electro-ion collisions drive the system towards equilibrium and maintain the equilibrium. However, the energy transfer between electrons and ions is very inefficient and their mutual equilibration is very slow. Therefore, we have electron and ion fluids of different temperatures for a relatively long time. There is nothing similar in QGP. There are heavy quarks - charm, bottom and top - which are, however, much less populated than the light quarks and gluons and their lifetime is short. Therefore, the heavy quarks hardly influence the QGP dynamics.

The electromagnetic plasma, which is the closest analogue of QGP, is the relativistic system of electrons, positrons and photons. Such a plasma is actually studied in context of some astrophysical applications, e.g. supernovae explosions. Then, the differences between QGP and EMP are of dynamical origin - the first one is governed by Quantum Chromodynamics while the second one by Quantum Electrodynamics. The former theory is Abelian while the later one is nonAbelian with a prominent role of gluons which carry color charges and thus, not only mediate the interaction among colored quarks and antiquarks but interact among themselves. Gluons, in contrast to photons, also contribute to the density of color charges and to the color current.

The most important common feature of EMP and QGP is the collective character of the dynamics. The range of electrostatic interaction is, in spite of the screening, usually much larger than the inter-particle spacing. There are many particles in the Debye sphere - the sphere of the radius equals the effective interaction range, and motion of these particles is highly correlated. There is a similar situation in the deconfined perturbative phase of QCD (7). The Debye mass is of order gT where g is the QCD constant and T is the temperature. Since the particle density in QGP is of order T^3, the number of partons in the Debye sphere, which is roughly $1/g^3$, is large in the weakly coupled ($1/g \gg 1$) QGP.

In various laboratory experiments, EMP is embedded in an external electromagnetic field. For example, the magnetic field is used to trap the plasma, and there are numerous fascinating phenomena occurring in such a situation. In the case of QGP produced in relativistic heavy-ion collisions, it is hard to imagine any external chromodynamic field applied to the plasma. Therefore, we will consider here only the systems where fields are self-consistently generated in the plasma.

Our article is organized as follows. Theoretical tools, which are used to describe the plasmas, are presented in Chapter 2. The tools include: the kinetic theory, the hydrodynamic approach and diagrammatic methods of field theory. In Chapter 3 we discuss collective phenomena which are the most characteristic feature of plasmas. After explaining the phenomenon of screening, quasi-particle modes in the equilibrium and non-equilibrium plasma are presented. We pay much attention to instabilities which crucially influence plasma dynamics. The problem of particle's energy loss in a plasma is also discussed. Chapter 4 is devoted to

the strongly coupled plasma which reveals particularly interesting properties.

Throughout the paper we use the natural units with $c = \hbar = k_B = 1$ and the metric $(1, -1, -1, -1)$. However, there is a little complication here. Plasma physicists usually use the Gauss (CGS) units, where the fine structure constant equals $\alpha = e^2 \approx 1/137$, while the electromagnetic counterpart of the units usually applied in QCD is the so-called Heaviside-Lorentz system where the 4π factor does not show up in the Maxwell equations but $\alpha = e^2/4\pi$. We stick to the traditionally used units in the two fields of physics, and thus the factor of 4π has to be additionally taken into account to compare EMP to QGP formulas.

2 THEORETICAL TOOLS

2.1 Transport theory

Transport theory provides a natural framework to study equilibrium and nonequilibrium plasmas. The central object of the theory is the distribution function which describes a time dependent distribution of particles in a phase-space spanned by the particle's momenta and positions. The distribution function of each plasma component evolves due to the inter-particle collisions and the interaction with an external and/or self-consistently generated mean-field. The two dynamical effects give rise to the collision and mean-field terms of a transport equation satisfied by the distribution function.

2.1.1 ELECTROMAGNETIC PLASMA A formulation of the kinetic theory of relativistic plasma can be found in (8). The distribution function is denoted as $f_n(\mathbf{p}, x)$ with the index n labeling plasma components: electrons, positrons, ions. Spin is usually treated as an internal degree of freedom. The function depends on the four-position $x \equiv (t, \mathbf{x})$ and the three-momentum $\mathbf{p}$. The four-momentum p obeys the mass-shell constraint $p^2 = m^2$, where m is the particle mass, and then $p \equiv (E_p, \mathbf{p})$ with $E_p \equiv \sqrt{m^2 + \mathbf{p}^2}$.

The distribution function satisfies the transport equation

$$\Big(p_\mu \partial^\mu + q_n p^\mu F_{\mu\nu} \partial_p^\nu\Big) f_n(\mathbf{p}, x) = C[f_n] \; , \tag{1}$$

where $C[f_n]$ denotes the collision term, q_n is the charge of the plasma species n and $F^{\mu\nu}$ is the electromagnetic strength tensor which either represents an external field applied to the system or/and is generated self-consistently by the four-currents present in the plasma

$$\partial^\mu F_{\mu\nu} = 4\pi j_\nu \; ,$$

where

$$j^\mu(x) = \sum_n q_n \int \frac{d^3p}{(2\pi)^3} \frac{p^\mu}{E_p} \, f_n(\mathbf{p}, x) \; . \tag{2}$$

The transport equation can be solved in the linear response approximation. The equation is linearized around the stationary and homogeneous state described by the distribution $\bar{f}_n(\mathbf{p})$. The state is also assumed to be neutral and there are no currents. The distribution function is then decomposed as

$$f_n(\mathbf{p}, x) = \bar{f}_n(\mathbf{p}) + \delta f_n(\mathbf{p}, x) \; ,$$

where $\bar{f}_n(\mathbf{p}) \gg \delta f_n(\mathbf{p}, x)$.

The transport equation linearized in δf_n and $F^{\mu\nu}$ can be exactly solved after the Fourier transformation, which is defined as

$$f(k) = \int d^4x \, e^{ikx} f(x) \; , \qquad f(x) = \int \frac{d^4k}{(2\pi)^4} \, e^{-ikx} f(k) \; . \tag{3}$$

Then, one finds $\delta f_n(\mathbf{p}, k)$, which is the Fourier transform of $\delta f_n(\mathbf{p}, x)$, and the induced current, which can be written as

$$\delta j^\mu(k) = -\Pi^{\mu\nu}(k) A_\nu(k) \; , \tag{4}$$

with the polarization tensor equal to

$$\Pi^{\mu\nu}(k) = 4\pi \sum_n q_n^2 \int \frac{d^3p}{(2\pi)^3} \bar{f}_n(\mathbf{p}) \, \frac{(p\cdot k)^2 g^{\mu\nu} + k^2 p^\mu p^\nu - (p\cdot k)(k^\mu p^\nu + k^\nu p^\mu)}{(p\cdot k)^2} \; . \tag{5}$$

The tensor is symmetric ($\Pi^{\mu\nu}(k) = \Pi^{\nu\mu}(k)$) and transverse ($k_\mu \Pi^{\mu\nu}(k) = 0$) which guarantees that the current given by Equation 4 is gauge independent.

For isotropic plasmas, the polarization tensor has only two independent components which are usually chosen as

$$\begin{aligned} \Pi_L(k) &= \Pi_{00}(k) \; , \\ \Pi_T(k) &= \frac{1}{2} \left(\delta_{ij} - \frac{k_i k_j}{\mathbf{k}^2} \right) \Pi_{ij}(k) \; , \end{aligned} \tag{6}$$

where the indices $i, j = 1, 2, 3$ label three-vector and tensor components. In the case of an ultrarelativistic ($T \gg m$) electron-positron equilibrium plasma, the momentum integral in Equation 5 can be performed analytically in the high-temperature limit ($T \gg \omega, |\mathbf{k}|$), and the result derived already in 1960 by Silin (9) reads

$$\begin{aligned} \Pi_L(k) &= -3\, m_\gamma^2 \left[1 - \frac{\omega}{2|\mathbf{k}|} \, \ln \frac{\omega + |\mathbf{k}|}{\omega - |\mathbf{k}|} \right] \; , \\ \Pi_T(k) &= \frac{3}{2} \, m_\gamma^2 \, \frac{\omega^2}{\mathbf{k}^2} \left[1 - \left(1 - \frac{\mathbf{k}^2}{\omega^2} \right) \frac{\omega}{2|\mathbf{k}|} \, \ln \frac{\omega + |\mathbf{k}|}{\omega - |\mathbf{k}|} \right] \; , \end{aligned} \tag{7}$$

where $k \equiv (\omega, \mathbf{k})$ and $m_\gamma \equiv eT/3$ denotes the *thermal photon mass* generated by the interaction of the photons with the electrons and positrons.

The above polarization tensor was found in the collisionless limit of the transport equation. The effect of collisions can be easily taken into account if the so-called BGK collision term is used in the transport equation (10). The result for an ultrarelativistic equilibrium plasma is given in (11).

2.1.2 QUARK-GLUON PLASMA The transport theory of QGP (12,13) appears to be much more complicated than its electromagnetic counterpart. The distribution function of quarks $Q(\mathbf{p}, x)$ is a hermitian $N_c \times N_c$ matrix in color space (for a SU(N_c) color gauge group). The distribution function is gauge dependent and it transforms under a local gauge transformation $U(x)$ as

$$Q(\mathbf{p}, x) \to U(x) \, Q(\mathbf{p}, x) \, U^\dagger(x) \; . \tag{8}$$

Here and in the most cases below, the color indices are suppressed. The distribution function of antiquarks, which we denote by $\tilde{Q}(\mathbf{p},x)$, is also a hermitian $N_c \times N_c$ matrix and it transforms according to Equation 8. The distribution function of gluons is a hermitian $(N_c^2-1)\times(N_c^2-1)$ matrix which transforms as

$$G(\mathbf{p},x) \to \mathcal{U}(x)\, G(\mathbf{p},x)\, \mathcal{U}^\dagger(x)\ , \tag{9}$$

where

$$\mathcal{U}_{ab}(x) = 2\mathrm{Tr}[\tau^a U(x) \tau^b U^\dagger(x)]\ ,$$

with $\tau^a,\ a=1,...,N_c^2-1$ being the $\mathrm{SU}(N_c)$ group generators in the fundamental representation with $\mathrm{Tr}(\tau^a\tau^b)=\frac{1}{2}\delta^{ab}$.

The color current is expressed in the fundamental representation as

$$\begin{aligned} j^\mu(x) = \ & - \ \frac{g}{2}\int \frac{d^3p}{(2\pi)^3}\, p^\mu \Big[Q(\mathbf{p},x) - \tilde{Q}(\mathbf{p},x) \\ & - \ \frac{1}{N_c}\mathrm{Tr}[Q(\mathbf{p},x) - \tilde{Q}(\mathbf{p},x)] + 2\tau^a \mathrm{Tr}[T^a G(\mathbf{p},x)]\Big]\ , \end{aligned} \tag{10}$$

where g is the QCD coupling constant. A sum over helicities, two per particle, and over quark flavors N_f is understood in Equation 10, even though it is not explicitly written down. The $\mathrm{SU}(N_c)$ generators in the adjoint representation are expressed through the structure constants $T^a_{bc} = -if_{abc}$, and are normalized as $\mathrm{Tr}[T^aT^b] = N_c\delta^{ab}$. The current can be decomposed as $j^\mu(x) = j^\mu_a(x)\tau^a$ with $j^\mu_a(x) = 2\mathrm{Tr}(\tau_a j^\mu(x))$. The distribution functions, which are proportional to the unit matrix in color space, are gauge independent and they provide the color current (Equation 10) which identically vanishes.

Gauge invariant quantities are given by the traces of the distribution functions. Thus, the baryon current and the energy-momentum tensor read

$$\begin{aligned} b^\mu(x) &= \frac{1}{3}\int \frac{d^3p}{(2\pi)^3}\, p^\mu\, \mathrm{Tr}\Big[Q(\mathbf{p},x) - \tilde{Q}(\mathbf{p},x)\Big]\ , \\ T^{\mu\nu}(x) &= \int \frac{d^3p}{(2\pi)^3}\, p^\mu p^\nu\, \mathrm{Tr}\Big[Q(\mathbf{p},x) + \tilde{Q}(\mathbf{p},x) + G(\mathbf{p},x)\Big]\ , \end{aligned}$$

where we use the same symbol $\mathrm{Tr}[\cdots]$ for the trace both in the fundamental and adjoint representations.

The distribution functions of quarks, antiquarks and gluons satisfy the transport equations:

$$p^\mu D_\mu Q(\mathbf{p},x) + \frac{g}{2}\, p^\mu \Big\{ F_{\mu\nu}(x), \partial_p^\nu Q(\mathbf{p},x)\Big\} = C[Q,\tilde{Q},G]\ , \tag{11}$$

$$p^\mu D_\mu \tilde{Q}(\mathbf{p},x) - \frac{g}{2}\, p^\mu \Big\{ F_{\mu\nu}(x), \partial_p^\nu \tilde{Q}(\mathbf{p},x)\Big\} = \tilde{C}[Q,\tilde{Q},G]\ , \tag{12}$$

$$p^\mu \mathcal{D}_\mu G(\mathbf{p},x) + \frac{g}{2}\, p^\mu \Big\{ \mathcal{F}_{\mu\nu}(x), \partial_p^\nu G(\mathbf{p},x)\Big\} = C_g[Q,\tilde{Q},G]\ , \tag{13}$$

where $\{...,...\}$ denotes the anticommutator and ∂_p^ν the four-momentum derivative[1]; the covariant derivatives D_μ and $\mathcal{D}_\mu$ act as

$$D_\mu = \partial_\mu - ig[A_\mu(x),...\,]\ , \qquad \mathcal{D}_\mu = \partial_\mu - ig[\mathcal{A}_\mu(x),...\,]\ ,$$

[1] As the distribution functions do not depend on p_0, the derivative over p_0 is identically zero.

with A_μ and $\mathcal{A}_\mu$ being four-potentials in the fundamental and adjoint representations, respectively:

$$A^\mu(x) = A^\mu_a(x)\tau^a \ , \qquad \mathcal{A}^\mu(x) = T^a A^\mu_a(x) \ .$$

The strength tensor in the fundamental representation is $F_{\mu\nu} = \partial_\mu A_\nu - \partial_\nu A_\mu - ig[A_\mu, A_\nu]$, while $\mathcal{F}_{\mu\nu}$ denotes the field strength tensor in the adjoint representation. $C, \tilde{C}$ and C_g represent the collision terms.

The transport equations are supplemented by the Yang-Mills equation describing generation of the gauge field

$$D_\mu F^{\mu\nu}(x) = j^\nu(x) \ , \tag{14}$$

where the color current is given by Equation 10.

As in the case of the EM plasma, the transport equations, which are linearized around a stationary, homogeneous and colorless state can be solved. Because of the color neutrality assumption, the analysis is rather similar to that of the Abelian plasma, and it ends up with the polarization tensor which is proportional to the unit matrix in the color space and has the form of Equation 5.

As in the case of EMP, the collisions can be easily taken into account using the approximate BGK collision terms (14,15). Within a more realistic approach color charges are treated in a similar way as spin degrees of freedom, and ones uses the so-called Waldmann-Snider collision terms (16, 17) which are usually applied to study spin transport.

2.2 Hydrodynamic approach

Within the hydrodynamic approach, the plasma is treated as a liquid and it is described in terms of macroscopic variables which obey the equations of motion resulting from the conservation laws. The fluid equations are applied to a large variety of plasma phenomena but, depending of the time scale of interest, the actual physical content of the equations is rather different.

Real hydrodynamics deals with systems which are in local equilibrium, and thus it is only applicable at sufficiently long time scales. The continuity and the Euler or Navier-Stokes equations are supplemented by the equation of state to form a complete set of equations. The equations can be derived from kinetic theory, using the distribution function of local equilibrium which by definition maximizes the entropy density, and thus, it cancels the collision terms of the transport equations.

In the electron-ion plasma there are several time scales of equilibration. The electron component of the plasma reaches the equilibrium in the shortest time, then ions are equilibrated but for a relatively long time the electron and ion temperatures remain different from each other, as the energy transfer between electrons to ions is rather inefficient. This happens due to the huge mass difference between electrons and ions.

When the electrons have reached local equilibrium with their own temperature and hydrodynamic velocity, the collision terms of the kinetic equations

representing electron-electron collisions vanish while the collision terms due to electron-ion collisions can be neglected as they influence the electron distribution function only at a sufficiently long time scale. Then, one obtains hydrodynamic equations of an electron fluid. When the ion component is also equilibrated we have two fluids with different temperatures and hydrodynamic velocities. At the times scales when the fluid equations are applicable, the plasma can be treated as locally neutral. Charge fluctuations are obviously possible but they disappear fast as the electric field generated by the local charges induces the currents which in turn neutralize the charges. Since the plasma is nearly an ideal conductor, the process of plasma neutralization is very fast. Due to the charge neutrality of the plasma, the electric field is not present in the fluid equations and we end up with the *magnetohydrodynamics* where the pressure gradients and magnetic field drive the plasma dynamics.

As explained above, the regime of magnetohydrodynamics appears because there is a heavy positive component of the plasma (ions) and a light negative component (electrons). There is no QCD analogue of magnetohydrodynamics as every quark or gluon can carry opposite color charges. Therefore, when local equilibrium is reached various color components of the plasma have the same temperatures and hydrodynamic velocities (17). Since the quark-gluon system becomes color neutral even before the local equilibration is reached (16, 14), we deal with hydrodynamics of neutral fluid where the chromodynamic fields are absent. Such a relativistic hydrodynamics of colorless QGP has been actively studied over the last two decades (18, 19).

The hydrodynamic equations, which actually express macroscopic conservation laws, hold not only for systems in local equilibrium but for systems out of equilibrium as well. The equations can be then applied at time scales significantly shorter than that of local equilibration. At such a short time scale, the collision terms of the transport equations can be neglected entirely. However, extra assumptions are then needed to close the set of equations, as the (equilibrium) equation of state cannot be used. Plasma physicists developed several methods to close the set of equations, and thus fluid equations are used to study bulk features of short time scale phenomena in the plasmas. To get more detailed information, the kinetic theory is needed. Since the fluid equations are noticeably simpler than the kinetic ones, the hydrodynamic approach is frequently used in numerical simulations of plasma evolution, studies of nonlinear dynamics, etc.

Below we derive the fluid equations for EMP and QGP from the respective kinetic theory. Since the fluid approach under consideration is supposed to hold at sufficiently short time scales, we use the collisionless transport equations.

2.2.1 ELECTROMAGNETIC PLASMA We assume here that there are several streams in the relativistic plasma system and that the distribution functions of each plasma component (electrons, positrons, ions) belonging of each stream satisfy the collisionless transport equation. The equations are coupled only through the electromagnetic mean field which is generated by the current coming from all streams. The field in turn interacts with every stream.

Integrating the collisionless transport Equation 1 over momentum, one finds

the continuity equation

$$\partial_\mu n^\mu_\alpha = 0 \; , \tag{15}$$

where the four-flow is

$$n^\mu_\alpha(x) \equiv \int \frac{d^3p}{(2\pi)^3} \; p^\mu f_\alpha(\mathbf{p}, x) \; . \tag{16}$$

The index α labels simultaneously the streams and plasma components.

Multiplying the transport Equation 1 by the four-momentum p and integrating it over momentum, we get

$$\partial_\mu T^{\mu\nu}_\alpha + q_\alpha n^\mu_\alpha F_\mu{}^\nu = 0 \; , \tag{17}$$

where the energy-momentum tensor is

$$T^{\mu\nu}_\alpha(x) \equiv \int \frac{d^3p}{(2\pi)^3} \; p^\mu p^\nu f_\alpha(\mathbf{p}, x) \; . \tag{18}$$

The structure of n^μ_α and $T^{\mu\nu}_\alpha$ is assumed to be that of the ideal fluid in local thermodynamic equilibrium. Thus, one has

$$n^\mu_\alpha(x) \;\; = \;\; n_\alpha(x) \, u^\mu_\alpha(x) \; , \tag{19}$$

$$T^{\mu\nu}_\alpha(x) \;\; = \;\; [\epsilon_\alpha(x) + p_\alpha(x)] u^\mu(x) u^\nu(x) - p_\alpha(x) \, g^{\mu\nu} \; . \tag{20}$$

To obtain the relativistic version of the Euler equation, Equation 17 needs to be manipulated following (20). Substituting the energy-momentum tensor of the form of Equation 20 into Equation 17 and projecting the result on the direction of u^μ_α, one finds

$$u_{\alpha\nu} \partial_\mu T^{\mu\nu}_\alpha = u^\mu_\alpha \partial_\mu \epsilon_\alpha + (\epsilon_\alpha + p_\alpha) \partial_\mu u^\mu_\alpha = 0 \; . \tag{21}$$

Computing $\partial_\mu T^{\mu\nu}_\alpha - u^\nu_\alpha u_{\alpha\rho} \partial_\mu T^{\mu\rho}_\alpha$, one gets the Lorentz covariant form of the Euler equation

$$M^\nu_\alpha \equiv (\epsilon_\alpha + p_\alpha) u_{\alpha\mu} \partial^\mu u^\nu_\alpha + (u^\mu_\alpha u^\nu_\alpha \partial_\mu - \partial^\nu) p - q_\alpha n_\alpha u_{\alpha\mu} F^{\mu\nu} = 0 \; . \tag{22}$$

The equation in a more familiar form is given by $\mathbf{M}_\alpha - \mathbf{v}_\alpha M^0_\alpha = 0$. Namely,

$$(\epsilon_\alpha + p_\alpha) \gamma^2_\alpha \Big(\frac{\partial}{\partial t} + \mathbf{v}_\alpha \cdot \nabla \Big) \mathbf{v}_\alpha + \Big(\nabla + \mathbf{v}_\alpha \frac{\partial}{\partial t} \Big) p_\alpha - q_\alpha n_\alpha \gamma_\alpha [\mathbf{E} - \mathbf{v}_\alpha (\mathbf{v}_\alpha \cdot \mathbf{E}) + \mathbf{v}_\alpha \times \mathbf{B}] = 0 \; , \tag{23}$$

where the four-velocity u^μ_α was expressed as $u^\mu_\alpha = (\gamma_\alpha, \gamma_\alpha \mathbf{v}_\alpha)$ with $\gamma_\alpha \equiv (1 - \mathbf{v}^2_\alpha)^{-1/2}$.

In the nonrelativistic limit (which is easily obtained when the velocity of light c is restored in the equation), Equation 23 gets the well-known form

$$\Big(\frac{\partial}{\partial t} + \mathbf{v}_\alpha \cdot \nabla \Big) \mathbf{v}_\alpha + \frac{1}{m_\alpha n_\alpha} \nabla p_\alpha - \frac{q_\alpha}{m_\alpha} (\mathbf{E} + \mathbf{v}_\alpha \times \mathbf{B}) = 0 \; . \tag{24}$$

The fluid Equations 15, 17 with n^μ_α and $T^{\mu\nu}_\alpha$ given by Equations 19, 20 do not constitute a closed set of equations - there are 5 equations and 6 unknown

functions: n_α, p_α, ϵ_α and 3 components of u^μ_α (because of the constraint $u^\mu_\alpha u_{\mu\,\alpha} = 1$, one component of u^μ_α can be eliminated). There are several methods to close the set of equations. In particular, assuming that the system's dynamics is dominated by the mean-field interaction, one can neglect the pressure gradients. One can also add an equation which relates p_α to ϵ_α. The relation is usually called the equation of state, but one should be aware that the plasma system is not in equilibrium, and the thermodynamic relations in general do not hold.

In the ultrarelativistic limit when the characteristic particle's energy (the temperature of the equilibrium system) is much larger than the particle's mass, and thus $p^2 = 0$, the energy-momentum tensor is traceless ($T^\mu_{\mu\,\alpha} = 0$), as follows from Equation 18 for $p^2 = 0$. Then, Equation 20 combined with the constraint $u^\mu_\alpha(x) u_{\alpha\,\mu}(x) = 1$ provides the desired relation

$$\epsilon_\alpha(x) = 3p_\alpha(x) \; , \tag{25}$$

which coincides with the equation of state of an ideal gas of massless particles.

Since the distribution functions of every plasma component belonging to every stream are assumed to obey the collisionless transport equation, we have a separated set of fluid equations for every plasma component of every stream. The equations are coupled only through the electromagnetic mean field. More precisely, the electrons, positrons and ions of every stream contribute to the current generating the field which in turn interacts with the streams.

The fluid equations can be solved in the linear response approximation. The equations are linearized around the stationary and homogeneous state described by $\bar{n}_\alpha$ and $\bar{u}^\mu_\alpha$. The state is neutral and there are no currents *i.e.*

$$\sum_\alpha \bar{n}_\alpha \bar{u}^\mu_\alpha = 0 \; . \tag{26}$$

The charge density is decomposed as

$$n_\alpha(x) = \bar{n}_\alpha + \delta n_\alpha(x) \; , \tag{27}$$

where $\bar{n}_\alpha \gg \delta n_\alpha$. The fully analogous decomposition of the hydrodynamic velocity u^μ_α, pressure p_α and energy density ϵ_α is also adopted.

The set of the continuity and Euler equations linearized in δn_α, δu^μ_α, δp_α, $\delta\epsilon_\alpha$, and $F^{\mu\nu}$ can be exactly solved after they are Fourier transformed. Thus, one finds $\delta n_\alpha(k)$, $\delta u^\mu_\alpha(k)$ when the set of fluid equations is closed by neglecting the pressure gradients. If the equation of state is used, one also finds $\delta\epsilon_\alpha(k)$.

Keeping in mind that the induced current equals

$$\delta j^\mu = \sum_\alpha (q_\alpha \bar{n}_\alpha \delta u^\mu_\alpha + q_\alpha \delta n_\alpha \, \bar{u}^\mu_\alpha) \; ,$$

one finds from Equation 4

$$\begin{aligned} \Pi^{\mu\nu}(k) \;\; &= \;\; \sum_\alpha \frac{4\pi q^2_\alpha \bar{n}^2_\alpha}{\bar{\epsilon}_\alpha + \bar{p}_\alpha} \, \frac{1}{(\bar{u}_\alpha \cdot k)^2} \Big[k^2 \bar{u}^\mu_\alpha \bar{u}^\nu_\alpha + (\bar{u}_\alpha \cdot k)^2 g^{\mu\nu} - (\bar{u}_\alpha \cdot k)(k^\mu \bar{u}^\nu_\alpha + k^\nu \bar{u}^\mu_\alpha) \\ &+ \;\; \frac{(\bar{u}_\alpha \cdot k) k^2 (k^\mu \bar{u}^\nu_\alpha + k^\nu \bar{u}^\mu_\alpha) - (\bar{u}_\alpha \cdot k)^2 k^\mu k^\nu - k^4 \bar{u}^\mu_\alpha \bar{u}^\nu_\alpha}{k^2 + 2(\bar{u}_\alpha \cdot k)^2} \Big] \; . \end{aligned} \tag{28}$$

The first term gives the polarization tensor when the pressure gradients are neglected while the second term gives the effect of the pressure gradients due to the equation of state given by Equation 25. The first term is symmetric ($\Pi^{\mu\nu}(k) = \Pi^{\nu\mu}(k)$) and transverse ($k_\mu \Pi^{\mu\nu}(k) = 0$). The second term is symmetric and transverse as well. Thus, the whole polarization tensor (Equation 28) is symmetric and transverse. The first term of Equation 28 can be obtained from the kinetic theory result (Equation 5) with the distribution function $\bar{f}_n(\mathbf{p})$ proportional to $\delta^{(3)}(\mathbf{p} - (\bar{\epsilon}_\alpha + \bar{p}_\alpha)\mathbf{u}_\alpha/\bar{n}_\alpha)$. Thus, the first term neglects the thermal motion of plasma particles while the second term takes the effect into account.

2.2.2 QUARK-GLUON PLASMA The fluid approach presented here follows the formulation given in (21). As in the EMP case, we assume that there are several streams in the plasma system and that the distribution functions of quarks, antiquarks and gluons of each stream satisfy the collisionless transport equation. The streams are labeled with the index α.

Further analysis is limited to quarks but inclusion of anti-quarks and gluons is straightforward. The distribution function of quarks belonging to the stream α is denoted as $Q_\alpha(\mathbf{p}, x)$. Integrating over momentum the collisionless transport Equation 11 satisfied by Q_α, one finds the covariant continuity equation

$$D_\mu n^\mu_\alpha = 0 \ , \tag{29}$$

where n^μ_α is $N_c \times N_c$ matrix defined as

$$n^\mu_\alpha(x) \equiv \int \frac{d^3p}{(2\pi)^3} \, p^\mu Q_\alpha(\mathbf{p}, x) \ . \tag{30}$$

The four-flow n^μ_α transforms under gauge transformations as the quark distribution function, *i.e.* according to Equation 8.

Multiplying the transport Equation 11 by the four-momentum and integrating the product over momentum, we get

$$D_\mu T^{\mu\nu}_\alpha - \frac{g}{2}\{F_\mu{}^\nu, n^\mu_\alpha\} = 0 \ , \tag{31}$$

where the energy-momentum tensor is

$$T^{\mu\nu}_\alpha(x) \equiv \int \frac{d^3p}{(2\pi)^3} \, p^\mu p^\nu Q_\alpha(\mathbf{p}, x) \ . \tag{32}$$

We further assume that the structure of n^μ_α and $T^{\mu\nu}_\alpha$ is

$$n^\mu_\alpha(x) = n_\alpha(x)\, u^\mu_\alpha(x) \ , \tag{33}$$

$$T^{\mu\nu}_\alpha(x) = \frac{1}{2}(\epsilon_\alpha(x) + p_\alpha(x))\{u^\mu_\alpha(x), u^\nu_\alpha(x)\} - p_\alpha(x)\, g^{\mu\nu} \ , \tag{34}$$

where the hydrodynamic velocity u^μ_α is, as n_α, ϵ_α and p_α, a $N_c \times N_c$ matrix. The anticommutator of u^μ_α and u^ν_α is present in Equation 34 to guarantee the symmetry of $T^{\mu\nu}_\alpha$ with respect to $\mu \leftrightarrow \nu$ which is evident in Equation 32.

In the case of an Abelian plasma, the relativistic version of the Euler equation is obtained from Equation 31 by removing from it the part which is parallel to

u^μ_α. An analogous procedure is not possible for the non-Abelian plasma because the matrices n_α, u^μ_α, and u^ν_α, in general, do not commute with each other. Thus, one has to work directly with Equations 29, 31 with n^μ_α and $T^{\mu\nu}_\alpha$ defined by Equations 33, 34. The equations have to be supplemented by the Yang-Mills Equation 14 with the color current of the form

$$j^\mu(x) = -\frac{g}{2}\sum_\alpha \left(n_\alpha u^\mu_\alpha - \frac{1}{N_c}\mathrm{Tr}[n_\alpha u^\mu_\alpha] \right) , \tag{35}$$

where only the quark contribution is taken into account.

The fluid Equations 29, 31, as their EM counter part, do not form a closed set of equations but can be closed analogously. The only difference is that the equation of state (Equation 25) relates to each other the matrix value functions ϵ_α and p_α.

As in the case of the EM plasma, the fluid Equations 15, 17, which are linearized around a stationary, homogeneous and colorless state described by $\bar{n}_\alpha$, $\bar{\epsilon}_\alpha$, $\bar{p}_\alpha$ and $\bar{u}^\mu_\alpha$, can be solved (21). Because of the color neutrality assumption, $\bar{n}_\alpha$, $\bar{\epsilon}_\alpha$, $\bar{p}_\alpha$ and $\bar{u}^\mu_\alpha$ are all proportional to the unit matrix in the color space, the analysis is rather similar to that of the Abelian plasma, and one ends up with the polarization tensor from Equation 28 which is proportional to the unit matrix in the color space.

2.3 Diagrammatic methods

Various characteristics of the weakly coupled plasma can be calculated using the perturbative expansion, that is diagrammatic methods of field theory. It requires a generalization of the Feynman rules applicable to processes, which occur in vacuum, to processes in many body plasma systems. When the plasma is in thermodynamical equilibrium one can either follow the so-called imaginary time formalism, see e.g. (22,23) or the real time (Schwinger-Keldysh) formalism (24,25). The latter can also be extended to non-equilibrium situations (26,27).

The perturbative expansion expressed in terms of Feynman diagrams allows one a systematic computation of various quantities. However, in order to obtain a gauge invariant finite result, one often has to resum a class of diagrams as required by the Hard Loop Approach (28,29,30) (the real-time formulation is discussed in (31)). The approach, which was first developed for equilibrium systems (28,29,30) (for a review see (32)) and then extended to the non-equilibrium case (33,34,35), distinguishes soft from hard momenta. In the case of ultrarelativitic QED plasmas in equilibrium, the soft momenta are of order eT while the hard momenta are of order T with T being the plasma temperature. One obviously assumes that $1/e \gg 1$. The Hard Loop Approach deals with soft collective excitations generated by hard plasma particles which dominate the distribution functions.

As an example, we consider the polarization tensor given by Equation 5, which was obtained within the kinetic theory in Sect. 2.1. We restrict ourselves to ultra-relativitic QED plasmas. In the lowest order of the perturbative expansion, the polarization tensor or photon self-energy is given by the diagram shown in Figure 1. The tensor can be decomposed into the vacuum and medium contributions.

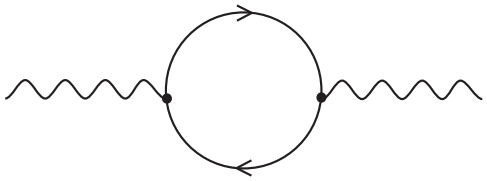


Figure 1: The lowest order contribution to the QED polarization tensor.

The first one requires an usual renormalization because of a ultraviolet divergence, whereas the medium part appears to be ultraviolet finite. One reproduces Equation 5 applying to the diagrammatic result the Hard Loop Approximation which requires that the energy and momentum (ω, $\mathbf{k}$) of the external photon line are much smaller than the momentum ($\mathbf{p}$) of the electron loop. Then, it appears that the vacuum part can be neglected, as it is much smaller than the medium part. In the case of an ultrarelativistic equilibrium EMP, Equations 7 were derived diagrammatically in (36,37). In QGP the lowest order polarization tensor (gluon self energy) includes one-loop diagrams with internal gluon and ghost lines. The final result for the gluon polarization tensor in the high-temperature approximation essentially coincides with the QED expression. The color degrees of freedom enter through the trivial color factor δ_{ab}. In the case of equilibrium QGP, one additionally replaces in Equation 7 the thermal photon mass by a thermal gluon mass given by

$$m_g^2 = \frac{g^2 T^2}{3} \left(1 + \frac{N_f}{6}\right) , \tag{36}$$

where N_f indicates the number of light quark flavors.

The Hard Loop Approach can be nicely formulated in terms of an effective action. Such an action for an equilibrium system was derived diagrammatically in (29) and in the explicitly gauge invariant form in (30). The equilibrium Hard Loop action was also found within the semiclassical kinetic theory (38,39). The action was generalized (33, 35) for non-equilibrium systems which, however, are on average locally color neutral, stationary and homogeneous.

The starting point was the effective action which describes an interaction of classical fields with currents induced by these fields in the plasma. The lagrangian density is quadratic in the gluon and quark fields and it equals

$$\mathcal{L}_2(x) = -\int d^4y \Big[\frac{1}{2} A^a_\mu(x) \Pi^{\mu\nu}_{ab}(x-y) A^b_\nu(y) + \bar{\Psi}(x) \Sigma(x-y) \Psi(y)\Big] , \tag{37}$$

where $\Pi^{\mu\nu}_{ab}$ and Σ is the gluon polarization tensor and the quark self-energy, respectively, while A^a and Ψ denote the gluon and quark fields. Following Braaten and Pisarski (30), the lagrangian from Equation 37 was modified to comply with the requirement of gauge invariance. The final result, which is non-local but manifestly gauge invariant, is

$$\begin{aligned} \mathcal{L}_{\rm HL}(x) = \frac{g^2}{2} \int \frac{d^3p}{(2\pi)^3} \quad \Big[& \quad f(\mathbf{p})\ F^a_{\mu\nu}(x) \Big(\frac{p^\nu p^\rho}{(p\cdot D)^2}\Big)_{ab} F_\rho^{\ b\mu}(x) \\ & + \quad i \frac{N_c^2 - 1}{4N_c} \tilde{f}(\mathbf{p})\ \bar{\Psi}(x) \frac{p\cdot\gamma}{p\cdot D} \Psi(x) \Big] , \end{aligned} \tag{38}$$

where $F_a^{\mu\nu}$ is the strength tensor and D denotes the covariant derivative; $f(\mathbf{p})$ and $\tilde{f}(\mathbf{p})$ are the effective parton distribution functions defined as $f(\mathbf{p}) \equiv n(\mathbf{p}) + \bar{n}(\mathbf{p}) + 2N_c n_g(\mathbf{p})$ and $\tilde{f}(\mathbf{p}) \equiv n(\mathbf{p}) + \bar{n}(\mathbf{p}) + 2n_g(\mathbf{p})$; $n(\mathbf{p})$, $\bar{n}(\mathbf{p})$ and $n_g(\mathbf{p})$ are the distribution functions of quarks, antiquarks and gluons of a single-color component in a homogeneous and stationary plasma which is locally and globally colourless; the spin and flavor are treated as parton internal degrees of freedom. The quarks and gluons are assumed to be massless. The effective action given by Equation 38 generates $n-$point functions which obey the Ward-Takahashi identities. Equation 38 holds under the assumption that the field amplitude is much smaller than T/g where T denotes the characteristic momentum of (hard) partons.

3 COLLECTIVE PHENOMENA

The most characteristic feature of the EM and QCD plasma, which results from a long range interaction governing both systems, is a collective behavior which leads to specific plasma phenomena like screening, plasma oscillations, instabilities, etc.

Since the electromagnetic and chromodynamic polarization tensors, which are obtained in the linear response analysis, are essentially the same, the collective effects in EMP and QGP are very similar in the linear response regime. As our discussion is limited to this regime, mostly the electromagnetic plasma is considered in this section.

3.1 Screening

We start with screening of electric charges in the plasma. To discuss the effect, let us consider an electric field generated by the point-like charge q moving with a velocity $\mathbf{v}$ in the plasma. The problem is studied in numerous plasma handbooks e.g. in (2). The induction vector obeys the Maxwell equation

$$\nabla \cdot \mathbf{D}(x) = 4\pi q \delta^{(3)}(\mathbf{r} - \mathbf{v}t) \ ,$$

with $x \equiv (t, \mathbf{r})$. After the Fourier transformation, which is defined by Equation 3, the induction vector reads

$$i\mathbf{k} \cdot \mathbf{D}(k) = 8\pi^2 q \ \delta(\omega - \mathbf{k} \cdot \mathbf{v}) \ , \tag{39}$$

where $k \equiv (\omega, \mathbf{k})$. The induction vector $\mathbf{D}(k)$ is related to the electric field $\mathbf{E}(k)$ through the dielectric tensor $\varepsilon^{ij}(k)$ as

$$D^i(k) = \varepsilon^{ij}(k) E^j(k) \ . \tag{40}$$

We note that the dielectric tensor $\varepsilon^{ij}(k)$, which carries information on the electromagnetic properties of a medium, can be expressed through the polarization tensor as

$$\epsilon^{ij}(k) = \delta^{ij} + \frac{1}{\omega^2} \Pi^{ij}(k) \ . \tag{41}$$

In the isotropic plasma there are only two independent components of the dielectric tensor ε_T and ε_L which are related to ε^{ij} as

$$\varepsilon^{ij}(k) = \varepsilon_T(k)\Big(\delta^{ij} - k^i k^j/\mathbf{k}^2\Big) + \varepsilon_L(k)\; k^i k^j/\mathbf{k}^2 \; . \tag{42}$$

Using Equations 40, 42, and expressing the electric field $\mathbf{E}$ through the scalar ϕ and vector $\mathbf{A}$ potentials ($\mathbf{E}(k) = -i\mathbf{k}\phi(k) + i\omega\mathbf{A}(k)$) in the Coulomb gauge ($\mathbf{k}\cdot\mathbf{A}(k) = 0$), one finds the electric potential in a medium (the wake potential)

$$\phi(x) = 4\pi q \int \frac{d^3k}{(2\pi)^3} \frac{e^{i\mathbf{k}(\mathbf{r}-\mathbf{v}t)}}{\varepsilon_L(\omega = \mathbf{v}\cdot\mathbf{k}, \mathbf{k})\; \mathbf{k}^2} \; . \tag{43}$$

Let us first consider the simplest case of the potential generated by a static ($\mathbf{v} = 0$) charge. Using Equations 6, 7, $\varepsilon_L(0, \mathbf{k})$ of an ultrarelatvistic electron-positron plasma is found as

$$\varepsilon_L(0, \mathbf{k}) = 1 + \frac{m_D^2}{\mathbf{k}^2} \; , \tag{44}$$

where m_D is the so-called Debye mass given by $m_D^2 = e^2T^2/3 = 3m_\gamma^2 = \Pi_L(0, \mathbf{k})$. Then, Equation 43 gives the well-known screened potential

$$\phi(\mathbf{r}) = \frac{q}{r}\, e^{-m_D r} \; , \tag{45}$$

with $r \equiv |\mathbf{r}|$. As seen, the inverse Debye mass has the interpretation of the screening length of the potential. Since the average inter-particle spacing in the ultrarelatvistic plasma is of order T^{-1}, the number of particles in the Debye sphere (the sphere of the radius m_D^{-1}) is of order e^{-3} which is, as already mentioned in the Introduction, much larger that than unity in the weakly coupled plasma ($1/e^2 \gg 1$). This explains the collective behavior of the plasma, as motion of particles from the Debye sphere is highly correlated.

For $\mathbf{v} \neq 0$ the potential given by Equation 43 has a rich structure. In the context of QGP it has been discussed in (40, 41, 42), showing that it can exhibit attractive contributions even between like-sign charges in certain directions (40). For a supersonic particle, the potential can reveal a Mach cone structure associated with Čerenkov radiation when electromagnetic properties of the plasma are appropriately modeled (41, 42).

3.2 Collective modes

Let us consider a plasma in a homogenous, stationary state with no local charges, no currents. As a fluctuation or perturbation of this state, there appear local charges or currents generating electric and magnetic fields which in turn interact with charged plasma particles. Then, the plasma reveals a collective motion which classically is termed as plasma oscillations. Quantum-mechanically we deal we quasi-particle collective excitations of the plasma.

The collective modes are found as solutions of the dispersion equation obtained from the equation of motion of the Fourier transformed electromagnetic potential $A^\mu(k)$ which is

$$\Big[k^2 g^{\mu\nu} - k^\mu k^\nu - \Pi^{\mu\nu}(k)\Big] A_\nu(k) = 0 \; , \tag{46}$$

where the polarization tensor $\Pi^{\mu\nu}$ contains all dynamical information about the system. The general dispersion equation is then

$$\det\Big[k^2 g^{\mu\nu} - k^\mu k^\nu - \Pi^{\mu\nu}(k)\Big] = 0\,. \tag{47}$$

Due to the transversality of $\Pi^{\mu\nu}(k)$ not all components of $\Pi^{\mu\nu}(k)$ are independent from each other, and consequently the dispersion Equation 47, which involves a determinant of a 4×4 matrix, can be simplified to the determinant of a 3×3 matrix. For this purpose one usually introduces the dielectric tensor $\varepsilon^{ij}(k)$ related to the polarization tensor by Equation 41. Then, the dispersion equation gets the form

$$\det\Big[\mathbf{k}^2\delta^{ij} - k^i k^j - \omega^2\varepsilon^{ij}(k)\Big] = 0\,. \tag{48}$$

The relationship between Equation 47 and Equation 48 is most easily seen in the Coulomb gauge when $\phi = 0$ and $\mathbf{k}\cdot\mathbf{A}(k) = 0$. Then, $\mathbf{E} = i\omega\mathbf{A}$ and Equation 46 is immediately transformed into an equation of motion of $\mathbf{E}(k)$ which further provides the dispersion Equation 48.

As expressed by Equation 42, there are only two independent components of the dielectric tensor ($\varepsilon_T(k)$ and $\varepsilon_L(k)$) in the isotropic plasma. Then, the dispersion Equation 48 splits into two equations

$$\varepsilon_T(k) = \mathbf{k}^2/\omega^2\,, \qquad \varepsilon_L(k) = 0\,. \tag{49}$$

Solutions of the dispersion equations $\omega(\mathbf{k})$, with a complex, in general, frequency ω, represent plasma modes which classically are, as already mentioned, the waves of electric and/or magnetic fields in the plasma while quantum-mechanically the modes are quasi-particle excitations of the plasma system. If the imaginary part of the mode's frequency $\Im\omega$ is negative, the mode is damped - its amplitude exponentially decays in time as $e^{\Im\omega t}$. When $\Im\omega = 0$ we have a stable mode with a constant amplitude. Finally, if $\Im\omega > 0$, the mode's amplitude exponentially grows in time - there is an instability.

When the electric field of a mode is parallel to its wave vector $\mathbf{k}$, the mode is called *longitudinal*. A mode is called *transverse* when the electric field is transverse to the wave vector. The Maxwell equations show that the longitudinal modes, also known as *electric*, are associated with electric charge oscillations; the transverse modes, also known as *magnetic*, are associated with electric current oscillations.

The collective (boson) modes in the equilibrium ultrarelativistic plasma are shown in Figure 2. There are longitudinal modes also called plasmons and transverse modes. Both start at zero momentum at the plasma frequency which is identical to the thermal photon (or gluon) mass, $\omega_p = m_\gamma$. The dispersion relations lies above the light cone ($\omega > |\mathbf{k}|$) showing that the plasma waves are undamped (no Landau damping) in the high-temperature limit. As explained in Sect. 3.3.1, the Landau damping, which formally arises from the imaginary part of the polarization tensor given by Equation 7 at $\omega^2 < \mathbf{k}^2$, occurs when the energy of the wave is transferred to plasma particles moving with velocity equal to the phase velocity ($\omega/|\mathbf{k}|$) of the wave. If the phase velocity is larger than the speed of light such a transfer is obviously not possible.

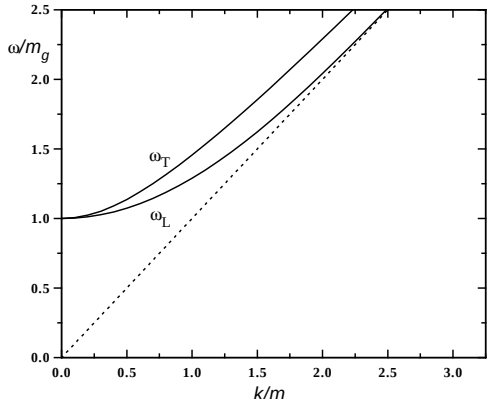


Figure 2: Dispersion relation of longitudinal and transverse plasma waves.

3.2.1 TWO-STREAM SYSTEM As an example of the rich spectrum of collective modes, we consider the two-stream system within the hydrodynamic approach when the effect of pressure gradients is neglected. Details of the analysis can be found in (21). The dielectric tensor provided by the polarization tensor from Equation 28 is

$$\varepsilon^{ij}(\omega,\mathbf{k}) = \Big(1-\frac{\omega_p^2}{\omega^2}\Big)\delta^{ij} - \frac{4\pi}{\omega^2}\sum_\alpha \frac{q_\alpha^2\bar{n}_\alpha^2}{\bar{\epsilon}_\alpha+\bar{p}_\alpha}\left[\frac{\bar{v}_\alpha^i k^j + \bar{v}_\alpha^j k^i}{\omega-\mathbf{k}\cdot\bar{\mathbf{v}}_\alpha} - \frac{(\omega^2-\mathbf{k}^2)\bar{v}_\alpha^i\bar{v}_\alpha^j}{(\omega-\mathbf{k}\cdot\bar{\mathbf{v}}_\alpha)^2}\right], \quad (50)$$

where $\bar{\mathbf{v}}_\alpha$ is the hydrodynamic velocity related to the hydrodynamic four-velocity $\bar{u}_\alpha^\mu$; ω_p is the plasma frequency given as

$$\omega_p^2 \equiv 4\pi\sum_\alpha \frac{q_\alpha^2\bar{n}_\alpha^2}{\bar{\epsilon}_\alpha+\bar{p}_\alpha}\,. \quad (51)$$

The index α, which labels the streams and plasma components, has four values, $\alpha = L-, L+, R-, R+$. The first character labels the stream ('R' for right and 'L' for left) while the second one labels the plasma component ('+' for positive and '−' for negative). For simplicity we assume here that the streams are neutral and identical to each other and their velocities, which are chosen along the axis z, are opposite to each other. Then,

$$\begin{aligned}
\bar{n} &\equiv \bar{n}_{L-} = \bar{n}_{L+} = \bar{n}_{R-} = \bar{n}_{R+}\,, \qquad \bar{\epsilon} \equiv \bar{\epsilon}_{L-} = \bar{\epsilon}_{L+} = \bar{\epsilon}_{R-} = \bar{\epsilon}_{R+}\,,\\
\bar{p} &\equiv \bar{p}_{L-} = \bar{p}_{L+} = \bar{p}_{R-} = \bar{p}_{R+}\,, \qquad \bar{v} \equiv \bar{v}_{L-} = \bar{v}_{L+} = -\bar{v}_{R-} = -\bar{v}_{R+}\,,\\
e &= q_{L-} = -q_{L+} = q_{R-} = -q_{R+}\,,
\end{aligned} \quad (52)$$

and the plasma frequency equals $\omega_p^2 = 16\pi e^2\bar{n}^2/(\bar{\epsilon}+\bar{p})$.

The wave vector is first chosen to be parallel to the axis x, $\mathbf{k} = (k,0,0)$. Due to Equations 52, the off-diagonal elements of the matrix in Equation 48 vanish and the dispersion equation with the dielectric tensor given by Equation 50 is

$$(\omega^2-\omega_p^2)(\omega^2-\omega_p^2-k^2)\Big(\omega^2-\omega_p^2-k^2-\lambda^2\,\frac{k^2-\omega^2}{\omega^2}\Big) = 0\,, \quad (53)$$

where $\lambda^2 \equiv \omega_p^2 \bar{v}^2$. As solutions of the equation, one finds a stable longitudinal mode with $\omega^2 = \omega_p^2$ and a stable transverse mode with $\omega^2 = \omega_p^2 + k^2$. There are also transverse modes with

$$\omega_\pm^2 = \frac{1}{2}\Big[\omega_p^2 - \lambda^2 + k^2 \pm \sqrt{(\omega_p^2 - \lambda^2 + k^2)^2 + 4\lambda^2 k^2}\Big] \,. \tag{54}$$

As seen, $\omega_+^2 > 0$ but $\omega_-^2 < 0$. Thus, the mode ω_+ is stable and there are two modes with pure imaginary frequency corresponding to $\omega_-^2 < 0$. The first mode is overdamped while the second one is the well-known unstable Weibel mode (43) leading to the filamentation instability. A physical mechanism of the instability is explained in Sect. 3.3.2.

The wave vector, as the stream velocities, is now chosen along the $z-$axis *i.e.* $\mathbf{k} = (0, 0, k)$. Then, the matrix in Equation 48 is diagonal. With the dielectric tensor given by Equation 50, the dispersion equation reads

$$(\omega^2 - \omega_p^2 - k^2)^2 \Big\{ \omega^2 - \omega_p^2 - \omega_p^2 \Big[\frac{k\bar{v}}{\omega - k\bar{v}} + \frac{(k^2 - \omega^2)\bar{v}^2}{2(\omega - k\bar{v})^2} - \frac{k\bar{v}}{\omega + k\bar{v}} + \frac{(k^2 - \omega^2)\bar{v}^2}{2(\omega + k\bar{v})^2} \Big] \Big\} = 0 \,. \tag{55}$$

There are two transverse stable modes with $\omega^2 = \omega_p^2 + k^2$. The longitudinal modes are solutions of the above equation which can be rewritten as

$$1 - \omega_0^2 \Big[\frac{1}{(\omega - k\bar{v})^2} + \frac{1}{(\omega + k\bar{v})^2} \Big] = 0 \,, \tag{56}$$

where $\omega_0^2 \equiv \omega_p^2 / 2\bar{\gamma}^2$ with $\bar{\gamma} = (1 - \bar{v}^2)^{-1/2}$. With the dimensionless quantities $x \equiv \omega/\omega_0$, $y \equiv k\bar{v}/\omega_0$, Equation 56 is

$$(x^2 - y^2)^2 - 2x^2 - 2y^2 = 0 \,, \tag{57}$$

and it is solved by

$$x_\pm^2 = y^2 + 1 \pm \sqrt{4y^2 + 1} \,. \tag{58}$$

As seen, x_+^2 is always positive and thus, it gives two real (stable) modes; x_-^2 is negative for $0 < y < \sqrt{2}$ and then, there are two pure imaginary modes. The unstable one corresponds to the two-stream electrostatic instability. A physical mechanism of the instability is explained in Sect. 3.3.1.

3.3 Instabilities

Presence of unstable modes in a plasma system crucially influences its dynamics. Huge difficulties encountered by the half-a-century program to built a thermonuclear reactor are just related to various instabilities experienced by a plasma which make the system's behavior very turbulent, hard to predict and hard to control.

There is a large variety of instabilities - the history of plasma physics is said to be a history of discoveries of new and new instabilities. Plasma instabilities can be divided into two general groups (1) *hydrodynamic* instabilities, caused by coordinate space inhomogeneities, (2) *kinetic* instabilities due to non-equilibrium momentum distribution of plasma particles.

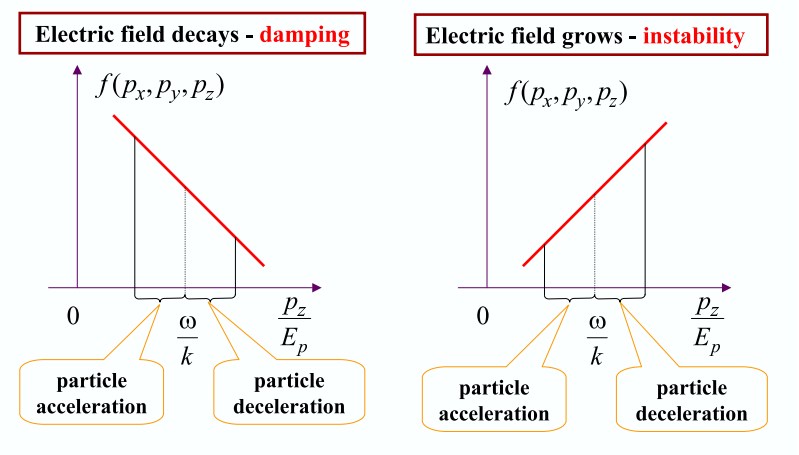


Figure 3: The mechanism of energy transfer between particles and fields.

The hydrodynamic instabilities are usually associated with phenomena occurring at the plasma boundaries. In the case of QGP, this is the domain of highly non-perturbative QCD where nonAbelian nature of the theory is of crucial importance. Then, the behavior of QGP is presumably very different from that of EMP, and thus, we will not speculate about possible analogies.

The kinetic instabilities are simply the collective modes with positive $\Im\omega$ introduced in Sect. 3.2 and found in Sect. 3.2.1 in the specific case of the two-stream system. Thus, we have longitudinal (electric) and transverse (magnetic) instabilities. In the non-relativistic plasma the electric instabilities are usually much more important than the magnetic ones, as the magnetic effects are suppressed by the factor v^2/c^2 where v is the particle's velocity. In the relativistic plasma both types of instabilities are of similar strength. As will be discussed later on, the electric instabilities occur when the momentum distribution of plasma particles has more than one maximum, as in the two-stream system. A sufficient condition for the magnetic instabilities appears to be an anisotropy of the momentum distribution.

3.3.1 MECHANISM OF ELECTRIC INSTABILITY Let us consider a plane wave of the electric field with the wave vector along the z axis. For a charged particle, which moves with a velocity $v = p_z/E_p$ equal to the phase velocity of the wave $v_\phi = \omega/k$, the electric field does not oscillates but it is constant. The particle is then either accelerated or decelerated depending on the field's phase. For an electron with $v = v_\phi$ chances to be accelerated and to be decelerated are equal to each other, as the time intervals spent by the particle in the acceleration zone and in the deceleration zone are equal to each other.

Let us now consider electrons with the velocities somewhat smaller the phase velocity of the wave. Such particles spend more time in the acceleration zone than in the deceleration zone, and the net result is that the particles with $v < v_\phi$ are accelerated. Consequently, the energy is transferred from the electric field to the particles. The particles with $v > v_\phi$ spend more time in the deceleration zone than in the acceleration zone, and thus they are effectively decelerated - the

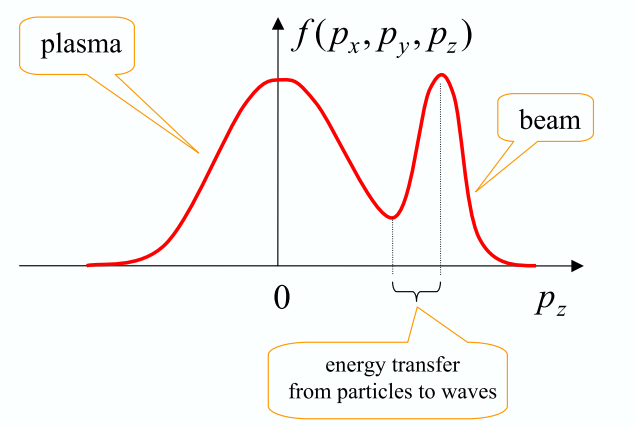


Figure 4: Momentum distribution of the plasma-beam system.

energy is transferred from the particles to the field. If the momentum distribution is such that there are more electrons in a system with $v < v_\phi$ than with $v > v_\phi$, the wave looses energy which is gained by the particles, as shown in the left-hand-side of Figure 3. This is the mechanism of famous collisionless Landau damping of the plasma oscillations. If there are more particles with $v > v_\phi$ than with $v < v_\phi$, the particles loose energy which is gained by the wave, as in the right-hand-side of Figure 3. Consequently, the wave amplitude grows. This is the mechanism of electric instability. As explained above, it requires the existence of the momentum interval where $f_n(\mathbf{p})$ grows with $\mathbf{p}$. Such an interval appears when the momentum distribution has more than one maximum. This happens in the two-stream system discussed in Sect. 3.2.1 or in the system of a plasma and a beam shown in Figure 4.

3.3.2 MECHANISM OF MAGNETIC INSTABILITY Since the magnetic instabilities appear to be relevant for QGP produced in relativistic heavy-ion collisions (see below), we discuss them in more detail. Let us first explain following (44), how the unstable transverse modes are initiated. For this purpose we consider a plasma system which is homogeneous but the momentum distribution of particles is not of the equilibrium form, it is *not* isotropic. The system is on average locally neutral ($\langle j^\mu(x)\rangle = 0$) but current fluctuations are possible, and thus the correlator $\langle j^\mu(x_1) j^\nu(x_2)\rangle$ is in general non-zero. Since the plasma is assumed to be weakly coupled, the correlator can be estimated neglecting the interaction entirely. Then, when the effects of quantum statistics are also neglected, the correlator equals

$$M^{\mu\nu}(t,\mathbf{x}) \stackrel{\text{def}}{=} \langle j^\mu(t_1,\mathbf{x}_1) j^\nu(t_2,\mathbf{x}_2)\rangle = \sum_n q_n^2 \int \frac{d^3p}{(2\pi)^3} \frac{p^\mu p^\nu}{E_p^2}\, f_n(\mathbf{p})\, \delta^{(3)}(\mathbf{x} - \mathbf{v}t)\ , \quad (59)$$

where $\mathbf{v} \equiv \mathbf{p}/E_p$ and $(t,\mathbf{x}) \equiv (t_2 - t_1, \mathbf{x}_2 - \mathbf{x}_1)$. Due to the average space-time homogeneity, the correlator given by Equation 59 depends only on the difference $(t_2 - t_1, \mathbf{x}_2 - \mathbf{x}_1)$. The space-time points $(t_1,\mathbf{x}_1)$ and $(t_2,\mathbf{x}_2)$ are correlated in the system of non-interacting particles if a particle travels from $(t_1,\mathbf{x}_1)$ to $(t_2,\mathbf{x}_2)$. For this reason the delta $\delta^{(3)}(\mathbf{x} - \mathbf{v}t)$ is present in Equation 59. The sum and

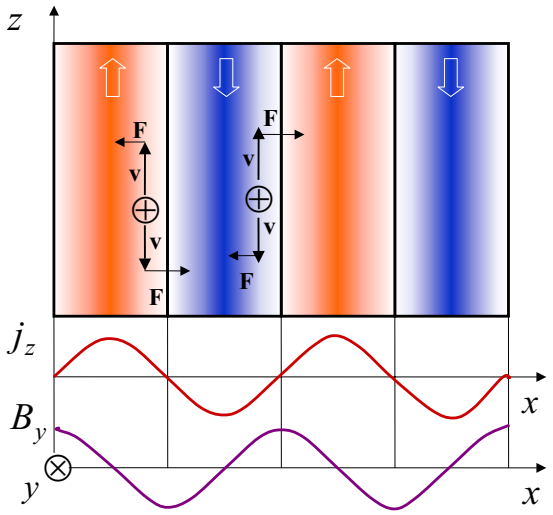


Figure 5: The mechanism of filamentation instability, see text for a description.

momentum integral represent summation over all particles in the system. The fluctuation spectrum is found as the Fourier transform of Equation 59 *i.e.*

$$M^{\mu\nu}(\omega,\mathbf{k}) = \sum_n q_n^2 \int \frac{d^3p}{(2\pi)^3}\,\frac{p^\mu p^\nu}{E_p^2}\; f_n(\mathbf{p})\; 2\pi\delta(\omega-\mathbf{kv})\;. \tag{60}$$

To further study the fluctuation spectrum, the particle's momentum distribution has to be specified. We will present here only a qualitative discussion of Equations 59, 60, assuming that the momentum distribution is strongly elongated in one direction which is chosen to be along the z axis. Then, the correlator M^{zz} is larger than M^{xx} or M^{yy}. It is also clear that M^{zz} is the largest when the wave vector $\mathbf{k}$ is along the direction of the momentum deficit, as in such a case the delta function $\delta(\omega-\mathbf{kv})$ does not much constrain the integral in Equation 60. Since the momentum distribution is elongated in the z direction, the current fluctuations are the largest when the wave vector $\mathbf{k}$ is the $x-y$ plane. Thus, we conclude that some fluctuations in the anisotropic system are large, much larger than in the isotropic one. An anisotropic system has a natural tendency to split into the current filaments parallel to the direction of the momentum surplus. These currents are seeds of the transverse unstable mode known as the filamentation or Weibel instability (43) which was found in the two-stream system discussed in Sect. 3.2.1.

Let us now explain in terms of elementary physics why the fluctuating currents, which flow in the direction of the momentum surplus, can grow in time. The form of the fluctuating current is chosen to be

$$\mathbf{j}(x) = j\;\hat{\mathbf{e}}_z\cos(k_x x)\;, \tag{61}$$

where $\hat{\mathbf{e}}_z$ is the unit vector in the z direction. As seen in Equation 61, there are current filaments of the thickness $\pi/|k_x|$ with the current flowing in the opposite directions in the neighboring filaments. The magnetic field generated by the

current from Equation 61 is given as

$$\mathbf{B}(x) = 4\pi \, \frac{j}{k_x} \, \hat{\mathbf{e}}_y \sin(k_x x) \; ,$$

and the Lorentz force acting on the particles, which fly along the z direction, equals

$$\mathbf{F}(x) = q \, \mathbf{v} \times \mathbf{B}(x) = -4\pi q \, v_z \, \frac{j}{k_x} \, \hat{\mathbf{e}}_x \sin(k_x x) \; ,$$

where q is the particle's electric charge. One observes, see Figure 5, that the force distributes the particles in such a way that those, which positively contribute to the current in a given filament, are focused in the filament center while those, which negatively contribute, are moved to the neighboring one. Thus, the initial current is growing and the magnetic field generated by this current is growing as well. The instability is driven by the the energy transferred from the particles to fields. More specifically, the kinetic energy related to the motion along the direction of the momentum surplus is used to generate the magnetic field.

3.3.3 ROLE OF INSTABILITIES As already mentioned, there is a large variety of plasma instabilities which strongly influence numerous plasma characteristics. Not much is known of the hydrodynamic instabilities of QGP and if they exist, they belong to the highly non-perturbative sector of QCD which is still poorly understood. As explained in Sect. 3.3.1, the electric instabilities occur in a two-stream system, or more generally, in systems with a momentum distribution of more than one maximum. While such a distribution is common in EMP, it is rather irrelevant for QGP produced in relativistic heavy-ion collisions where the global as well as local momentum distribution is expected to monotonously decrease in every direction from the maximum. The electric instabilities are absent in such a system but a magnetic unstable mode, which has been discussed in Sect. 3.3.2, is possible. The filamentaion instability was first argued to be relevant for the QGP produced in relativistic heavy-ion collisions in (45, 46, 44). A characteristic time of instability growth was estimated (45, 46) to be shorter or at least comparable to other time scales of the parton system evolution. The mechanism of instability growth was also clarified (44). The early arguments were substantiated in the forthcoming analytic calculations (47,48,49) and numerical simulations (50, 51, 52, 53, 54).

A main consequence of instabilities is a fast equilibration of the weakly coupled plasma. The problem is of particular interest as the experimental data on heavy-ion collisions, where QGP production is expected, suggest that an equilibration time of the parton system is below 1 fm/c (55). A whole scenario of instabilities driven equilibration is reviewed in (56). Here we only mention the main points, starting with an observation that collisions of charged particles are not very efficient in redistributing particle momenta, as the Rutherford cross section is strongly peaked at a small momentum transfer. One either needs many frequent but soft collisions or a few rare but hard collisions to substantially change a particle's momentum. As a result the inverse time of collisional equilibration of QGP is of order $g^4 \ln(1/g) \, T$ (16) where T is the characteristic momentum of

quarks or gluons. It appears that the momentum distribution is isotropized due to instabilities within the inverse time of order gT (57). If $1/g \gg 1$, the collisional equilibration is obviously much slower. As discussed in Chapter 4, the situation changes in strongly-coupled plasmas.

When the instabilities grow, the system becomes more and more isotropic (46,57) because the Lorentz force changes the particle's momenta and the growing fields carry an extra momentum. To explain the mechanism let us assume that initially there is a momentum surplus in the z direction. The fluctuating current flows in the z direction with the wave vector pointing in the x direction. Since the magnetic field has a y component, the Lorentz force, which acts on partons flying along the z axis, pushes the partons in the x direction where there is a momentum deficit. The numerical simulation (52) shows that growth of the instabilities is indeed accompanied with the system's fast isotropization.

The system isotropizes not only due to the effect of the Lorentz force but also due to the momentum carried by the growing field. When the magnetic and electric fields are oriented along the y and z axes, respectively, the Poynting vector points in the direction x that is along the wave vector. Thus, the momentum carried by the fields is oriented in the direction of the momentum deficit of particles.

Although the scenario of instabilities driven equilibration looks very promising, the problem of thermalization of QGP produced in heavy-ion collisions is far from being settled. It has been shown (58) that inter-parton collisions, which have been modeled using the BGK collision term (10), reduce the growth of instabilities and thus slow down the process of equilibration. The equilibration is also slowed down due to expansion of QGP into vacuum (59, 60) which is a characteristic feature of QGP produced in relativistic heavy-ion collisions. Finally, the late stage of instability development, when nonAbelian effects are crucially important, appears to be very complex (61, 62) and it is far from being understood.

As already mentioned, instabilities influence various plasma characteristics. In particular, it is known (63) that turbulent magnetic fields generated in the systems, which are unstable with respect to transverse modes, are responsible for a reduction of plasma viscosity. Then, an anomalously small viscosity, which is usually associated with strongly coupled systems, can occur in weakly coupled plasmas as well. Recently, it has been argued (64, 65) that the mechanism of viscosity reduction is operative in the unstable QGP.

3.4 Energy loss

A charged particle which moves across the plasma changes its energy due to several processes (2). When the particle's energy (E) is comparable to the plasma temperature (T), the particle can gain energy due to interactions with field fluctuations. (In context of QGP the problem was studied in (68).) A fast particle with $E \gg T$ looses its energy and main contributions come from collisions with other plasma particles and from radiation. In the following we discuss the energy loss of a fast particle, as the problem is closely related to jet quenching which was suggested long ago as a signature for the QGP formation in relativistic heavy-ion

collisions (66, 67).

Let us start with the collisional energy loss. The particle's collisions are split into two classes: *hard* with high-momentum transfer, corresponding to the collisions with plasma particles and, *soft* with low-momentum transfer dominated by the interactions with plasma collective modes. The momentum is called 'soft' when it is of order of the Debye mass, m_D, or smaller and it is 'hard' when it is larger than m_D.

The soft contribution to the energy loss, which can be treated in a classical way, is often called the process of plasma polarization. It leads to the energy loss per unit time given by the formula

$$\left(\frac{dE}{dt}\right)_{\rm soft} = \int d^3x\, \mathbf{j}(x)\mathbf{E}(x)\ , \tag{62}$$

where $\mathbf{E}$ is the electric field induced in the plasma by the particle's current $\mathbf{j}$ which is of the form $\mathbf{j}(x) = q\mathbf{v}\delta^{(3)}(\mathbf{x}-\mathbf{v}t)$. The field can be calculated by means of the Maxwell equations. After eliminating the magnetic field, one finds the equation

$$\left[\varepsilon^{ij}(k) - \frac{\mathbf{k}^2}{\omega^2}\left(\delta^{ij} - \frac{k^i k^j}{\mathbf{k}^2}\right)\right] E_j(k) = \frac{4\pi}{i\omega}\, j^i(k)\ .$$

Since we consider equilibrium plasma, which is isotropic, one introduces the longitudinal (ε_L) and transverse (ε_L) components of ε^{ij}. Then, Equation 62 is manipulated to

$$\left(\frac{dE}{dx}\right)_{\rm soft} = -\frac{4\pi i e^2}{v}\int \frac{d^3k}{(2\pi)^3}\left\{\frac{\omega}{\mathbf{k}^2\varepsilon_L(k)} + \frac{\mathbf{v}^2-\omega^2/\mathbf{k}^2}{\omega[\epsilon_T(k)-\mathbf{k}^2/\omega^2]}\right\}\ , \tag{63}$$

which gives the energy loss per unit length. This formula describes the effect of medium polarization. However, three comments are in order here.

1. Equation 63 includes the charge self-interaction signaled by the ultraviolet divergence of the integral from Equation 63. The self-interaction is removed by subtracting from Equation 63 the vacuum expression with $\varepsilon_L = \varepsilon_T = 1$.
2. Poles of the function under the integral Equation 63 correspond to the plasma collective modes as given by the dispersion Equations 49. Therefore, the explicit expressions of ε_L and ε_L are not actually needed to compute the integral in Equation 63. The knowledge of the spectrum of quasiparticles appears to be sufficient.
3. Equation 63 is derived in the classical approximation which breaks down for a sufficiently large $\mathbf{k}$. Therefore, an upper cut-off is needed. The interaction with $\mathbf{k}$ above the cut-off, which, as already mentioned, is of order of the Debye mass, should be treated as hard collisions with plasma particles.

The energy loss per unit length due to hard collisions is

$$\left(\frac{dE}{dx}\right)_{\rm hard} = \sum_i \int \frac{d^3k}{(2\pi)^3}\ n_i(k)\ [\text{flux factor}] \int d\Omega \frac{d\sigma^i}{d\Omega}\nu\ , \tag{64}$$

where the sum runs over particle species distributed according to $n_i(k)$, $\nu \equiv E - E'$ is the energy transfer, and $d\sigma^i/d\Omega$ is the respective differential cross section.

Combining Equations 63 and 64, one finds the complete collisional energy loss. The calculations of the energy loss of a fast parton in the QGP along the lines presented above were performed in (69, 70). Systematic calculations of the collisional energy loss using the Hard Thermal Loop resummation technique were given in (72, 71) with a result which is infrared finite, gauge invariant, and complete to leading order. Recently, the calculations of the collisional energy loss have been extended to anisotropic QGP (73).

It was realized that a sizeable contribution to the quark's energy loss comes from radiative processes (74). The problem, however, appeared to be very complex because quark's successive interactions in the plasma cannot be treated as independent from each other and there is a destructive interference of radiated gluons known as the Landau-Pomeranchuk-Migdal effect (75). There are numerous papers devoted to the radiative energy loss and the whole problem is reviewed in (76). A general conclusion of these studies is that the energy lost by a fast light quark quadraticaly (not linearly) depends on the path traversed in QGP, as the radiative energy loss dominates over the collisional. Recent experiments at RHIC show (77, 78), however, that heavy quarks, whose radiative energy loss is significantly suppressed, are strongly dragged in the QGP medium. It may suggest that the collisional energy loss should be actually enhanced as theoretically predicted in (79).

4 STRONGLY COUPLED PLASMAS

Our discussion of the collective phenomena presented in Sect. 3 was limited to the weakly interacting plasmas with the coupling constant much smaller than unity. However, QGP produced in ultrarelativistic heavy-ion collisions is presumably strongly coupled (sQGP) as the temperature is never much larger than $\Lambda_{\rm QCD}$, and the regime of asymptotic freedom is not reached. QGP is certainly a strongly interacting system close to the confinement phase transition. There are indeed hints in the extensive experimental material collected at RHIC (80,81,82,83) that the matter produced at the early stage of nucleus-nucleus collisions RHIC is in the form of sQGP for a few fm/c. In particular, the characteristics of elliptic flow and particle spectra, which are described well by ideal hydrodynamics, seem to indicate a fast thermalization and small viscosity of the plasma. Both features are naturally explained assuming a strong coupling of the plasma (55, 84, 85, 86, 87).

Although a fast thermalization (56) as well as a small viscosity (64,65) can also be explained by instabilities, the idea of sQGP certainly needs to be examined. However, the theoretical tools presented in Chapter 2 implicitly or explicitly assume small coupling constant and they are of limited applicability. A powerful approach, which can be used to study sQGP is the lattice formulation of QCD, for a review see (88). However, lattice QCD calculations, which are mostly numerical, encounter serious problems to incorporate quark degrees of freedom. It is also very difficult to analyze time dependent plasma characteristics.

Strongly coupled conformal field theories such as supersymmetric QCD can be studied by means of the so-called AdS/CFT duality (89). Although some very interesting results on the conformal QGP were obtained in this way, see e.g. (90) and references therein, relevance of these results for QGP governed by QCD, not by supersymmetric QCD, is unclear. Thus, the question arises what we can learn about sQGP from strongly coupled EMP.

We first note that most of EMP in nature and technological applications are weakly coupled i.e. the interaction energy between the plasma particles is much smaller than their thermal (kinetic) energy. This is because strongly coupled plasmas require a high particle density and/or low temperature, at which usually strong recombination occurs and the plasma state vanishes. Exceptions are the ion component in white dwarfs, metallic hydrogen and other states of dense warm matter in the interior of giant planets, short-living dense plasmas produced by intense laser or heavy ion beams or in explosive shock tubes, dusty (or complex) plasmas, and two-dimensional electron systems on liquid helium (91,92,93). Therefore, it is a real challenge to study strongly coupled EMP both theoretically and experimentally.

In nonrelativistic EMP the interaction energy is given by the (screened) Coulomb potential. The Coulomb coupling parameter defined by

$$\Gamma = \frac{q^2}{a\,T} \tag{65}$$

distinguishes between weakly coupled, $\Gamma \ll 1$, and strongly coupled plasmas, $\Gamma \gtrsim 1$. Here q is the particle charge, a the interparticle distance and T the kinetic temperature of the plasma component (electrons, ions, charged dust grains) under consideration. In the case of a degenerate plasma, e.g. the electron component in a white dwarf, the kinetic energy T is replaced by the Fermi energy. Due to the strong interaction, the plasma can behave either as a gas or a liquid or even a solid (crystalline) system.

The case of an one-component plasma (OCP) with a pure Coulomb interaction (a single species of charged particles in an uniform, neutralizing background) has been studied as a reference model for strongly coupled plasmas using simple models as well as numerical simulations in great detail (91). For $\Gamma > 172$ the plasma was shown to form regular structures (Coulomb crystallization) (94). Below this critical value the OCP is in the supercritical state. For values of Γ larger than about 50, it behaves like an ordinary liquid, while for small values below unity like a gas. Only if Γ is large enough, the usual liquid behavior (Arrhenius law for the viscosity, Stokes-Einstein relation between self-diffusion and shear viscosity, etc.) appears due to caging of the particles (a single particle is trapped for some period of time in the cage formed by its nearest neighbors). For values of Γ, which are smaller than about 50, caging is not sufficiently strong and the system shows complicated, not yet understood transport properties. However, the short-range ordering typical for liquids shows up already for $\Gamma > 3$ (95). A gas-liquid transition, requiring a long-range attraction and a short-range repulsion, e.g. Lennard-Jones potential, does not exist in the OCP with particles of like-sign charges.

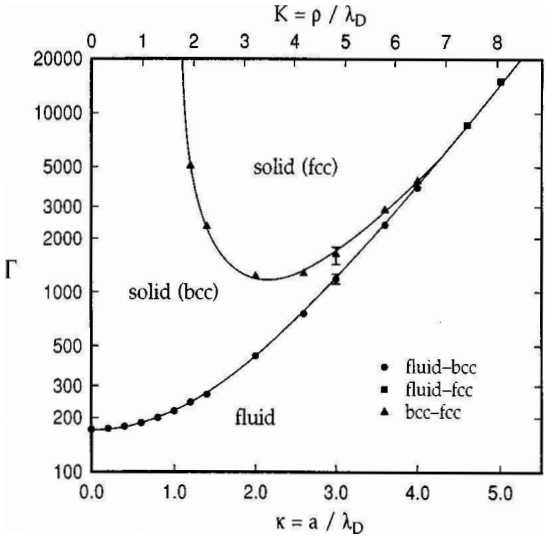


Figure 6: Phase diagram of a strongly coupled Yukawa system from Ref. (96).

In realistic systems with a screened Coulomb interaction (Yukawa potential), the phase diagram can be shown in the Γ-κ-plane, where $\kappa = a/\lambda_D$ is the distance parameter with λ_D being the Debye screening length. Numerical simulations based on molecular dynamics lead to the phase diagram shown in Figure 6 (96).

The first quantity of interest of sQGP is the coupling parameter. In analogy to nonrelativistic EMP, it is defined as (97)

$$\Gamma = \frac{2Cg^2}{4\pi a\, T} = 1.5 - 5, \tag{66}$$

where C is the Casimir invariant ($C = 4/3$ for quarks and $C = 3$ for gluons), $a \simeq 0.5$ fm is the interparticle distance, and $T \simeq 200$ MeV is the QGP temperature corresponding to a strong coupling constant $g \simeq 2$. The factor 2 in the numerator comes from taking into account the magnetic interaction in addition to the static electric (Coulomb) interaction, which are of the same magnitude in ultrarelativistic plasmas. The factor 4π in the denominator comes from using the Heavyside-Lorentz system in QCD as discussed in the Introduction. The distance parameter κ of the QGP under the above conditions is rather small, typically between 1 and 3 (98).

It should be noted, that we have assumed here a classical interaction potential corresponding to a one-gluon exchange. However, an effective potential taking into account higher order and non-perturbative effects may be much larger. This might be related to the fact that experimental data suggest a cross section enhancement for the parton interaction by more than an order of magnitude (see below). Hence the effective coupling parameter might be up to an order of magnitude larger than Equation 66.

As discussed above, comparison to the OCP model as well as experimental data suggest that QGP close to the confinement phase transition could be in a liquid phase. So, the question arises whether there is a phase transition from a liquid to a gaseous QGP, as sketched in Figure 7. For such a transition, a

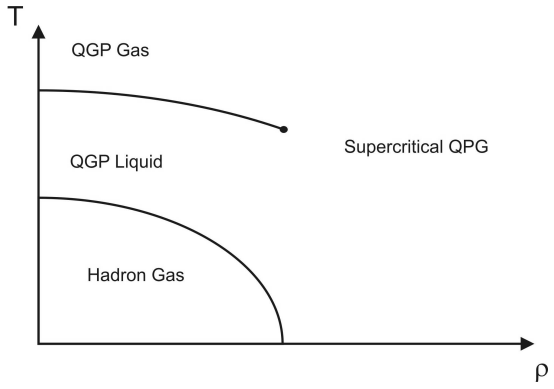


Figure 7: Sketch of a phase diagram of strongly interacting matter with a possible gas-liquid transition in the QGP phase. T denotes the temperature while ρ is the baryon density.

Lennard-Jones type interaction between the partons is required. However, the parton interaction in perturbative QCD is either purely repulsive or attractive in the various interaction channels, e.g quark-antiquark or diquark channel. Due to non-linear effects caused by the strong coupling, however, attractive interactions can arise even in the case like-sign charges (see e.g. (99)) leading to Lennard-Jones type potentials. Hence a gas-liquid transition in QGP with a critical point, proposed in (87), is not excluded and deserves further investigation.

An important quantity, which is very useful in theoretical and experimental studies of strongly coupled systems on the microscopic level, in particular in fluid physics (100), are correlation functions. In particular, the pair correlation function and the static structure function provide valuable information on the equation of state of the system (100). The extension of the approach to the QGP has been proposed in (98).

The static density-density autocorrelation function is defined for a classical system as (100, 91)

$$G(\mathbf{r}) = \frac{1}{N} \int d^3r' \, \langle \rho(\mathbf{r}+\mathbf{r}',t)\, \rho(\mathbf{r}',t) \rangle,$$

where N is the total number of particles and

$$\rho(\mathbf{r},t) = \sum_{i=1}^{N} \delta^{(3)}(\mathbf{r} - \mathbf{r}_i(t))$$

is the local density of point particles with $\mathbf{r}_i(t)$ denoting the position of $i-$th particle at time t. The density-density autocorrelation function is related to the pair correlation function, which is defined as

$$g(\mathbf{r}) = \frac{1}{N} \, \langle \sum_{i,j,i\neq j}^{N} \delta^{(3)}(\mathbf{r} + \mathbf{r}_i - \mathbf{r}_j) \rangle,$$

by the relation $G(\mathbf{r}) = g(\mathbf{r}) + \delta^{(3)}(\mathbf{r})$. The static structure function, defined by

$$S(\mathbf{p}) = \frac{1}{N} \, \langle \rho(\mathbf{p}) \rho(-\mathbf{p}) \rangle$$

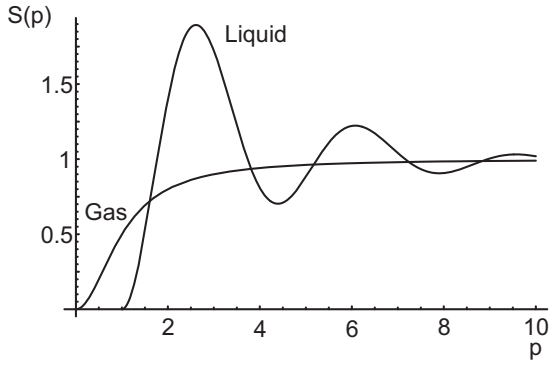


Figure 8: Sketch of the static structure functions vs. momentum in the gas and liquid phase in arbitrary units.

with the Fourier transformed particle density,

$$\rho(\mathbf{p}) = \int d^3r\, \rho(\mathbf{r})\, e^{-i\mathbf{p}\cdot\mathbf{r}},$$

is the Fourier transform of the density-density autocorrelation function

$$S(\mathbf{p}) = \int d^3r\, e^{-i\mathbf{p}\cdot\mathbf{r}} G(\mathbf{r})\,.$$

The static structure function $S(\mathbf{p})$ is constant for $\mathbf{p} \neq 0$ for uncorrelated particles (2). The typical behavior of the function in an interacting gas and in a liquid is sketched in Figure 8. The oscillatory behavior is caused by short range correlations, corresponding to a short range ordering typical for liquids. In the case of OCP, the oscillations appear for $\Gamma > 3$ indicating a liquid behavior (albeit with non-standard transport properties) of the supercritical phase already for rather low values of Γ (95).

The static quark structure function can be related to the longitudinal gluon polarization tensor containing only the quark loop (Figure 1) via

$$S(\mathbf{p}) = -\frac{12}{\pi g^2 n} \int_0^\infty d\omega\, \Im\Pi_L(\omega, \mathbf{p})\, \coth\frac{\omega}{2T},$$

where $n = N/V = \langle\rho(\mathbf{r})\rangle$ is the average particle density in a homogeneous system. As a reference for the strong coupling regime, the static quark structure function has been calculated in the weak coupling limit by resumming the polarization tensor in the high-temperature limit (Equation 7) leading to (98)

$$S(\mathbf{p}) = \frac{2N_f T^3}{n} \frac{\mathbf{p}^2}{\mathbf{p}^2 + m_D^2}, \tag{67}$$

where $m_D^2 = N_f g^2 T^2/6$ is the quark contribution to the Debye screening mass. The static structure function given by Equation 67 starts at zero for $|\mathbf{p}| = 0$ and saturates at the uncorrelated structure function $S(\mathbf{p}) = 2N_f T^3/n$ for large $|\mathbf{p}|$. Such a structure function corresponds to an interacting Yukawa system in the gas phase (see Figure 8). Indeed, the pair correlation function, following from

the Fourier transform of $S(\mathbf{p}) - 1$, is

$$g(r) = -\frac{N_f T^3}{2\pi n} \frac{m_D^2}{r} e^{-m_D r},$$

and it reproduces the Yukawa potential.

In order to compute the structure function in strongly-coupled plasmas, molecular dynamics is used (91). Although QGP is not a classical system, as the thermal de Broglie wave length is of the same order as the interparticle distance, molecular dynamics might be useful as a first estimate (87). Using molecular dynamics for a classical sQGP (101, 102, 103), the expected behavior described above has been qualitatively verified (101). In strongly coupled dense matter, where quantum effects are important, quantum molecular dynamics based on a combination of classical molecular dynamics with the density functional theory has been successfully applied (104). A generalization to the relativistic QGP has not been attempted so far. As an ultimate choice, lattice QCD could be used to calculate the structure or pair correlation functions. This would provide a test for the state of sQGP as well as the importance of quantum effects by comparing lattice results to classical molecular simulations.

As a last application, we consider the influence of strong coupling on the cross sections entering transport coefficients (shear viscosity), stopping power, and other dynamical quantities of the plasma. Beside higher-order and non-perturbative quantum effects, there is already a cross section enhancement on the classical level. The reason is that the Coulomb radius, defined as $r_c = q^2/E$ with the particle energy E, is of the order of the Debye screening length or r_c is even larger than λ_D in a strongly coupled plasma. Hence the standard Coulomb scattering formula has to be modified since the interaction with particles outside of the Debye sphere contributes significantly, and consequently the inverse screening length cannot be used as an infrared cutoff. This modification leads, for example, to the experimentally observed enhancement of the so-called ion drag force in complex plasmas which is caused by the ion-dust interaction (105).

In the QGP at $T \simeq 200$ MeV, the ratio r_c/λ_D equals 1 - 5. It might enhance a parton cross section by a factor of 2 - 9 (97) compared to perturbative results. An enhanced cross section reduces the mean free path λ, and consequently it reduces the viscosity η as $\eta \sim \lambda$. An enhancement of the elastic parton cross section by more than an order of magnitude compared to perturbative results also explains the elliptic flow and particle spectra observed at RHIC (106). An infrared cutoff smaller than the Debye mass gives a natural explanation for this enhancement. We also note that if the cross section is enhanced, the collisional energy loss grows. On the other hand, the radiative energy loss is expected to be suppressed in the strongly coupled QGP by the Landau-Pomeranchuk-Migdal effect (75).

Finally, we mention two examples of strongly coupled systems which have not been considered in QGP physics but may be of relevance. Strongly coupled plasmas such as two-dimensional Yukawa liquids (107) and dusty plasmas are non-Newtonian fluids, i.e. the shear viscosity depends on the shear rate (flow velocity) as it is well known in daily life from ketchup (shear thinning). The

second example concerns nanofluidics. The expanding fireball in ultrarelativistic heavy-ion collisions has a transverse dimension of about 20 inter-particle distances (about 10 fm). Fluids consisting of such a low number of layers exhibit properties different from large fluid systems. For example, the shear flow does not show an continuous velocity gradient but jumps due to the adhesive forces between two layers. Such an behavior has been observed for example in complex plasmas.

LITERATURE CITED

1. Krall NA, Trivelpiece AW. *Principles of Plasma Physics.* New Yrok: McGraw-Hill (1973)
2. Ichimaru S. *Basic Principles of Plasma Physics.* Reading: Benjamin (1973)
3. *Quark-Gluon Plasma*, ed. RC Hwa. Singapore: World Scientific (1990)
4. *Quark-Gluon Plasma 2,* ed. RC Hwa. Singapore: World Scientific (1995)
5. *Quark-Gluon Plasma 3*, eds. RC Hwa, XN Wang. Singapore: World Scientific (2004)
6. Mrówczyński St. *Acta Phys. Polon. B* 29:3711 (1998)
7. Blaizot JP, Iancu E. *Phys. Rept.* 359:355 (2002)
8. deGroot SR, Van Leeuwen WA, van Weert ChG. *Relativistic Kinetic Theory.* Amsterdam: North-Holland (1980)
9. Silin VP. *Sov. Phys. JETP* 11:1136 (1960)
10. Alexandrov AF, Bogdankovich LS, Rukhadze AA. *Principles of Plasma Electrodynamics.* Berlin: Springer (1984)
11. Carrington ME, Fugleberg T, Pickering D, Thoma MH. *Can J. Phys.* 82:671 (2004)
12. Elze HT, Heinz UW. *Phys. Rept.* 183:81 (1989)
13. Mrówczyński St. *Phys. Rev. D* 39:1940 (1989)
14. Manuel C, Mrówczyński St. *Phys. Rev. D* 70:094019 (2004)
15. Schenke B, Strickland M, Greiner C, Thoma MH. *Phys. Rev. D* 73:125004 (2006)
16. Arnold P, Son DT, Yaffe LG. *Phys. Rev. D* 59:105020 (1999)
17. Manuel C, Mrówczyński St. *Phys. Rev. D* 68:094010 (2003)
18. Kolb PF, Heinz UW. In *Quark Gluon Plasma 3*, eds. RC Hwa, XN Wang, p. 634. Singapore: World Scientific (2004)
19. Huovinen P, Ruuskanen PV. *Ann. Rev. Nucl. Part. Sci.* 56:163 (2006)
20. Landau LD, Lifshitz EM. *Fluid Mechanics.* Oxford: Pergamon (1963)
21. Manuel C, Mrówczyński St. *Phys. Rev. D* 74:105003 (2006)
22. Kapusta JI. *Finite-Temperature Field Theory.* Cambridge: Cambridge University Press (1989)
23. Le Bellac M. *Thermal Field Theory.* Cambridge: Cambridge University Press (1996)
24. Schwinger JS. *J. Math. Phys.* 2:407 (1961)
25. Keldysh LV. *Zh. Eksp. Teor. Fiz.* 47:1515 (1964) [*Sov. Phys. JETP* 20:1018 (1965)]
26. Kadanoff LP, Baym G. *Quantum Statistical Mechanics.* New York: Benjamin (1962)
27. Bezzerides B, Dubois DF. *Ann. Phys.* 70:10 (1972)
28. Braaten E, Pisarski RD. *Nucl. Phys. B* 337:569 (1990)
29. Taylor JC, Wong SMH. *Nucl. Phys. B* 346:115 (1990)
30. Braaten E, Pisarski RD. *Phys. Rev. D* 45:1827 (1992)
31. Carrington ME, Hou D, Thoma MH. *Eur. Phys. J. C* 7:347 (1999)
32. Thoma MH. In *Quark-Gluon Plasma 2,* ed. RC Hwa, p. 51. Singapore: World

Scientific (1995)
33. Pisarski RD. hep-ph/9710370 (1997)
34. Mrówczyński St, Thoma MH. *Phys. Rev. D* 62:036011 (2000)
35. Mrówczyński St, Rebhan A, Strickland M. *Phys. Rev. D* 70:025004 (2004)
36. Klimov VV. *Sov. Phys. JETP* 55:199 (1982)
37. Weldon HA. *Phys. Rev. D* 26:1394 (1982)
38. Blaizot JP, Iancu E. *Nucl. Phys. B* 417:608 (1994)
39. Kelly PF, Liu Q, Lucchesi C, Manuel C. *Phys. Rev. D* 50:4209 (1994)
40. Mustafa MG, Thoma MH, Chakraborty P. *Phys. Rev. C* 71:017901 (2005)
41. Ruppert J, Müller B. *Phys. Lett. B* 618:123 (2005)
42. Chakraborty P, Mustafa MG, Thoma MH. *Phys. Rev. D* 74:094002 (2006)
43. E.S. Weibel, *Phys. Rev. Lett.* 2:83 (1959)
44. Mrówczyński St. *Phys. Lett. B* 393:26 (1997)
45. Mrówczyński St. *Phys. Lett. B* 314:118 (1993)
46. Mrówczyński St. *Phys. Rev. C* 49:2191 (1994)
47. Randrup J, Mrówczyński St. *Phys. Rev. C* 68:034909 (2003)
48. Romatschke P, Strickland M. *Phys. Rev. D* 68:036004 (2003)
49. Arnold P, Lenaghan J, Moore GD. *JHEP* 0308:002 (2003)
50. Rebhan A, Romatschke P, Strickland M. *Phys. Rev. Lett.* 94:102303 (2005)
51. Arnold P, Lenaghan J. *Phys. Rev. D* 70:114007 (2004)
52. Dumitru A, Nara Y. *Phys. Lett. B* 621:89 (2005)
53. Arnold P, Moore GD, Yaffe LG. *Phys. Rev. D* 72:054003 (2005)
54. Rebhan A, Romatschke P, Strickland M. *JHEP* 0509:041 (2005)
55. Heinz U. *AIP Conf. Proc.* 739:163 (2005)
56. Mrówczyński St. *Acta Phys. Polon. B* 37:427 (2006)
57. Arnold P, Lenaghan J, Moore GD, Yaffe LG. *Phys. Rev. Lett.* 94:072302 (2005)
58. Schenke B, Strickland M, Greiner C, Thoma MH. *Phys. Rev. D* 73:125004 (2006)
59. Romatschke P, Venugopalan R. *Phys. Rev. Lett.* 96:062302 (2006)
60. Romatschke P, Rebhan A. *Phys. Rev. Lett.* 97:252301 (2006)
61. Arnold P, Moore GD. *Phys. Rev. D* 73:025013 (2006)
62. Dumitru A, Nara Y, Strickland M. hep-ph/0604149 (2006)
63. Abe T and Niu K. *J. Phys. Soc. Jap.* 49:717 (1980)
64. Asakawa M, Bass SA, Müller B. *Phys. Rev. Lett.* 96:252301 (2006)
65. Asakawa M, Bass SA, Müller B. hep-ph/0608270 (2006)
66. Bjorken JD. *Fermilab preprint* 82/59-THY (1982)
67. Gyulassy M, Plümer M. *Phys. Lett. B* 243:432 (1990)
68. Chakraborty P, Mustafa MG, Thoma MH. hep-ph/0611355 (2006)
69. Thoma MH, Gyulassy M. *Nucl. Phys. B* 351:491 (1991)
70. Mrówczyński St. *Phys. Lett B* 269:383 (1991)
71. Braaten E, Thoma MH. *Phys. Rev. D* 44:R2625 (1991)
72. Braaten E, Thoma MH. *Phys. Rev. D* 44:1298 (1991)
73. Romatschke P, Strickland M. *Phys. Rev. D* 71:125008 (2005)
74. Gyulassy M, Wang XN. *Nucl. Phys. B* 420:583 (1994)

75. Landau LD, Pomeranchuk IY. *Dokl. Akad. Nauk. SSR* 92:535 (1953); Landau LD, Pomeranchuk IY. *Dokl. Akad. Nauk. SSR* 92:735 (1953); Migdal AB. *Phys. Rev.* 103:1811 (1956).
76. Baier R, Schiff D, Zakharov BG. *Ann. Rev. Nucl. Part. Sci.* 50:37 (2000)
77. Adler SS, et al. (PHENIX Collab.) *Phys. Rev. Lett.* 96:032301 (2006)
78. Abelev BI, et al. (STAR Collab.) nucl-ex/0607012 (2006)
79. Mustafa MG, Thoma MH. *Acta Phys. Hung. A* 22:93 (2005)
80. Arsene I, et al. (BRAHMS Collab.) *Nucl. Phys. A* 757:1 (2005)
81. Back BB, et al. (PHOBOS Collab.) *Nucl. Phys. A* 757:28 (2005)
82. Adams J, et al. (STAR Collab.) *Nucl. Phys. A* 757:102 (2005)
83. Adcox K, et al. (PHENIX Collab.) *Nucl. Phys. A* 757:184 (2005)
84. Gyulassy M, McLerran L. *Nucl. Phys. A* 750:30 (2005)
85. Shuryak EV. *Nucl. Phys. A* 774:387 (2006)
86. Cassing W, Peshier A. *Phys. Rev. Lett.* 94:172301 (2005)
87. Thoma MH. *Nucl. Phys. A* 774:307 (2006)
88. Karsch F. *Lect. Notes Phys.* 583:209 (2002)
89. Maldacena JM. *Adv. Theor. Math. Phys.* 2:231 (1998) [*Int. J. Theor. Phys.* 38:1113 (1999)]
90. Kovtun P, Son DT, Starinets AO. *Phys. Rev. Lett.* 94:111601 (2005); Janik RA, Peschanski R. *Phys. Rev. D* 74:046007 (2006)
91. Ichimaru S. *Rev. Mod. Phys.* 54:1017 (1982)
92. Fortov VE, et al. *Phys. Rept.* 421:1 (2005)
93. Tahir NA, et al. *J. Phys. A: Math. Gen.* 39:4755 (2006); Hoffmann DHH, et al., *J. Phys. IV* 133:49 (2006)
94. Slattery WL, Doolen GD, Witt HE. *Phys. Rev. A* 21:2087 (1980)
95. Daligault J. *Phys. Rev. Lett.* 96:065003 (2006)
96. Hamaguchi S, Farouki RT, Dubin DHE. *Phys. Rev. E* 56:4671 (1997)
97. Thoma MH. *J. Phys. G* 31:L7 (2005); Erratum. *J. Phys. G* 31:539 (2005)
98. Thoma MH. *Phys. Rev. D* 72:094030 (2005)
99. Tsytovich V. *Contrib. Plasma Phys.* 45:533 (2005)
100. Hansen JP, McDonald IR. *Theory of Simple Liquids.* London: Academic Press (1986)
101. Gelman BA, Shuryak EV, Zahed I. *Phys. Rev. C* 74:044908 (2006)
102. Gelman BA, Shuryak EV, Zahed I. *Phys. Rev. C* 74:044909 (2006)
103. Hartmann P, Donko Z, Levai P, Kalman GJ. *Nucl. Phys. A* 774:881 (2006)
104. Car R, Parrinello M. *Phys. Rev. Lett.* 55:2471 (1985)
105. V. Yaroshenko, et al. *Phys. Plasmas* 12:093503 (2005)
106. Molnar D, Gyulassy M. *Nucl. Phys. A* 697:495 (2002)
107. Donko Z, Goree J, Hartmann P, Kutasi K. *Phys. Rev. Lett.* 96:145003 (2006)